Experimental study on the energy absorption capability of circular corrugated tubes under lateral loading and axial loading

Original Article

Institution of MECHANICAL ENGINEERS
Journal of AUTOMOBILE ENGINEERING

Proc IMechE Part D:
J Automobile Engineering
2015, Vol. 229(13) 1739–1761

DOI: 10.1177/0954407014568130
pid.sagepub.com
SAGE

Experimental study on the energy absorption capability of circular corrugated tubes under lateral loading and axial loading

Abbas Niknejad[1], Yashar Abdolzadeh[1], Jafar Rouzegar[2] and Mohammad Abbasi[1]

Abstract

A new type of energy absorber called an expansion joint (i.e. a corrugated tube) is examined in this research. Several experiments are performed on three types of thin-walled specimen, namely circular tubes, preformed corrugated tubes and complete corrugated tubes, to investigate the energy absorption of steel specimens under different conditions for quasi-static lateral loading and axial loading. For this purpose, some steel specimens were compressed between two rigid platens in the axial direction, and the other specimens were laterally compressed. The preformed corrugated tubes and the complete corrugated tubes were produced by the hydroforming method. In each geometrical group of specimens, several tubes, which have different wall thicknesses, different inner diameters and different lengths and which are either empty or filled with polyurethane foam, were tested. Experiments show that, for a lateral load, the specific absorbed energies of the complete corrugated tubes are higher than those of the corresponding preformed corrugated tubes and circular tubes with the same characteristics. Tests show that, under lateral loading, a complete corrugated tube with a thicker wall and a smaller diameter is the optimum energy absorber system. Therefore, when a circular tube transforms into the corrugated tube, a better energy absorber system with a higher capability is achieved under lateral loading. Also, experiments show that, under axial loading, simple circular tubes with no forming process have higher specific absorbed energies than corrugated tubes do. Corrugated specimens have more controllable plastic deformation and a more regular deformation mode than simple tubes have. Tests under axial loading illustrate that, when the preformed corrugated tubes are filled with polyurethane foam, the specific absorbed energy increases by up to 74%. A comparison of the results on empty and filled specimens shows that, in some cases, the specific absorbed energies of corrugated tubes under lateral loading are higher than the specific absorbed energies of circular tubes under axial loading. This means that, by shaping the circular tubes into preformed corrugated tubes and complete corrugated tubes via the hydroforming process, a new thin-walled structure with a high specific absorbed energy during the lateral compression process is introduced.

Keywords

Absorbed energy, axial compression, corrugated tubes, lateral compression, polyurethane foam, thin-walled structures

Date received: 8 June 2014; accepted: 18 December 2014

Introduction

The safety of passengers in every kind of vehicle is the most important parameter in the designing process of the vehicle structure. The best way to achieve this goal is to dissipate the kinetic energy outside the vehicle cabin by considering some energy absorber system. Much attention has been paid to thin-walled structures as energy-absorbing systems because of their capability and adaptability. Round tubes which collapse progressively in an axisymmetric mode, a diamond mode or a mixed mode are very good energy absorbers and, consequently, several experimental and analytical studies

[1]Mechanical Engineering Department, Yasouj University, Yasouj, Iran
[2]Mechanical and Aerospace Engineering Department, Shiraz University of Technology, Shiraz, Iran

Corresponding author:
Abbas Niknejad, Mechanical Engineering Department, Yasouj University, PO Box 75914–353, Yasouj, Iran.
Email: Aniknejad@yu.ac.ir

have been devoted to understand the mechanics of deformation during their collapse.[1] Wu and Carney[2] prepared a series of experiments on elliptical tubes with various ratios of the semi-axes to study the initial collapse behaviour of braced elliptical tubes. Niknejad et al.[3] studied plastic deformation of axially compressed hexagonal columns by numerical, theoretical and experimental methods. Guillow et al.[4] prepared some experiments on thin-walled circular aluminium tubes. They found that the ratio of the maximum load to the average load increased substantially with increasing diameter-to-wall thickness ratio. Abramowicz[5] presented basic examples of the design process of typical energy-absorbing components to calculate and design thin-walled components for optimal impact energy dissipation. Huang et al.[6] investigated the energy-absorbing behaviour of axially splitting and curling square mild steel and aluminium tubes. Both quasi-static tests and dynamic tests were conducted. A simple quasi-static kinematics model was developed which describes all the main features of the deformation process. Marsolek and Reimerdes[7] investigated the influences of different induced folding modes to optimize the energy absorption behaviour of axially loaded metallic cylindrical shells. Also, they found that the initial force peak significantly decreased by triggering non-axisymmetric folding patterns. The axial impact of thin-walled tubes with square cross-sections, which incorporate axial stiffeners, was studied by Jones et al.[8] The collapse behaviour and the crashworthiness characteristics of cantilevered circular tubes subjected to bending were studied by Mamalis et al.[9] both theoretically and experimentally. Three different fixture devices were used and their effects on the failure behaviour of the tubes was investigated in detail. Morris et al.[10] conducted experimental and numerical investigations of the lateral compression of nested circular metal tubes to achieve maximum energy absorption. Different variations in the external constraints were used to increase the energy-absorbing capacities of these nested systems. Olabi et al.[11] performed an overview of mild steel and aluminium tubes during the energy absorption process subjected to axial compression, lateral compression, indentation and inversion. Experimental investigations were carried out on three different geometrical types of composite tube, namely radial corrugated composite tubes, cylindrical composite tubes and corrugated surrounded cylindrical tubes, by Abdewi et al.[12] to study the effect of the corrugation geometry. Their results showed that the load-carrying capability is significantly influenced by the corrugation geometry in axial crushing. Mahdi and El Kadi[13] evaluated predictions of both the load-carrying capacities and the energy absorption capabilities of glass fibre–epoxy composite tubes with an elliptical cross-section under lateral loading, using artificial neural networks. Aktay et al.[14] studied the axial folding process on empty structures and structures filled with polystyrene and aluminium foam filler with hexagonal and square packing configurations in the quasi-static condition by experimental and numerical methods. Olabi et al.[15] performed an experimental study on two types of nested circular energy absorber subjected to dynamic lateral compression by a drop-weight machine.

Poonaya et al.[16] developed a closed-form solution of thin-walled circular tubes subjected to bending by using a rigid-plastic mechanism analysis. Niknejad et al.[17] performed a theoretical analysis and estimated the diagram of the axial compression load versus the displacement of rectangular and square columns in the polyurethane-foam-filled condition. Fan et al.[18] investigated experimentally the lateral crushing behaviour of sandwich tubes and also revealed and classified different crushing patterns of sandwich tubes under lateral compression. Niknejad et al.[19] experimentally studied the effects of the tube length, the wall thickness, the diameter and also the presence of polyurethane foam filler on the plastic deformation of circular metal tubes under quasi-static lateral loading. Niknejad et al.[20] estimated the mean axial load during the quasi-static folding process on circular grooved tubes filled with polyurethane foam. Mahdi and Hamouda[21] examined the effects of the hexagonal angle, the packing system and the loading direction on the crushing behaviour, the absorbed energy, the failure mode and the failure mechanism of composite hexagonal rings. Obradovic et al.[22] presented numerical simulations of the axial impact event for the lightweight frontal safety structure of the Formula SAE vehicle designed by the Politecnico di Torino team. Alavi Nia and Parsapour[23] showed that, in 3×3 square tubes with unequal cells, adding the partitions at the corners increases the energy absorption capacity of the tubes. Martinez et al.[24] found that, in the axial crushing of expanded tubes, the peak load and the energy absorption capacity depend on the number of expanded metal cells in the cross-section. Mahdi et al.[25] investigated the effects of the fibre orientation on the energy absorption capability of composite tubes. Eyvazian et al.[26] showed that axially compressed tubes with corrugations have a uniform load versus displacement curve without an initial peak load. Hong et al.[27] suggested a theoretical model to predict the strength of multi-cell tubes with triangular lattices. Their research claimed that lattice tubes have mean crushing forces about 60–103% higher than those of single-cell tubes.

This article investigates and compares the plastic deformation of circular tubes, preformed corrugated tubes and corrugated tubes in the empty condition and the polyurethane-foam-filled condition under quasi-static axial loading and lateral compression loading between two rigid platens. The corrugated specimens were produced by the hydroforming method. The effects of the initial form, the initial diameter, the wall thickness and the foam filler of the specimens on the energy absorption characteristics of the specimens under axial loading and lateral loading are studied.

Experiments

Test specimens were made from steel E304 by the hydroforming method. The specimens were prepared in three geometrical groups of thin-walled specimens, namely circular tubes, preformed corrugated tubes and complete corrugated tubes, and were used in quasi-static lateral compression and axial compression tests. To study the influences of the geometrical characteristics of the specimens on the energy absorption behaviour, the specimens were prepared with different diameters and different wall thicknesses. For each geometrical condition, two similar specimens were prepared, and one of these specimens was filled with polyurethane foam to investigate the influence of the filler. Experimental diagrams of the axial load, the lateral load and the absorbed energy versus displacement of each specimen were drawn. The three geometrical types of specimen are illustrated in Figure 1. Also, Figure 2 shows some specimens filled with polyurethane foam. All the specimens were compressed between two rigid platens in a DMG machine, model 7166. The geometrical properties and the masses of the empty specimens and the foam-filled specimens for the lateral tests are reported in Table 1 and Table 2 respectively. Also, Table 3 and Table 4 give the same information on the empty specimens and the foam-filled specimens respectively for the axial tests. In the tables, R_i, t, L, m and r_e are the inner radius, the wall thickness, the length, the mass and the corrugation radius respectively of the preformed corrugated tubes and the complete corrugated tubes. Figure 3 illustrates the geometrical parameters of the corrugated specimens. All the lateral compression tests and the axial compression tests were performed at a loading rate of 10 mm/min. Three similar specimens of each case were provided and compressed to confirm the repeatability of the experiments.

Results and discussion

Based on the experimental results, the effects of the geometrical shape, the diameter, the wall thickness, the polyurethane foam filler and the loading types (axial and lateral) on the plastic deformation and the energy absorption of the specimens are studied.

Lateral compression

According to the lateral compression tests on the simple circular tubes, the preformed corrugated tubes and the complete corrugated tubes, the effects of the geometrical shape, the diameter and the wall thickness of the tube on the lateral load and the absorbed energy of the specimens are discussed for both the empty condition and the filled condition.

Effects of tube form. Figure 4 illustrates the experimental diagrams of the lateral load per unit of specimen mass versus the lateral displacement of the empty specimens LE-54, LE-47 and LE-45 and the corresponding graphs of the filled specimens LF-85, LF-89 and LF-92. In each compared group, the above-mentioned specimens have the same wall thicknesses and the same inner diameters. The empty specimens LE-54, LE-47 and LE-45 are a complete corrugated tube, a preformed corrugated tube and a circular tube respectively. Also, the filled specimens LF-85 and LF-89 are a complete corrugated tube and a preformed corrugated tube respectively, and specimen LF-92 is a simple tube. Figure 4 shows that, through the flattening process on the empty specimens and the polyurethane-foam-filled specimens, the complete corrugated tube has the highest lateral load, and the circular tube has the lowest lateral load. Therefore, the complete corrugated tube has a higher lateral load during the lateral compression process and, when a higher level of force is required, a complete corrugated tube is a better choice.

Experimental observations show that, during the flattening process on the specimens, two plastic hinge lines are created at the left side and the right side of the tubes, and the specimen wall rotates around these plastic hinge lines; therefore, a local bending occurs at the plastic hinges. During the bending process of a plate around a straight hinge line, the moment of inertia of the local cross-section around the neutral axis is the main factor of the plate strength against the bending deformation. During the shaping process of circular tubes into complete corrugated tubes by the hydroforming method, the inertia moment of the longitudinal cross-section of the tube wall increases markedly; therefore, the lateral load of the flattening process of a corrugated specimen is considerably higher than that of the corresponding simple tube. In order to reach a better conclusion, Figure 5 compares two slabs with the same thickness t and the same length L as the longitudinal cross-sections of the wall of the simple tube and the corrugated specimen. According to the figure, the inertia moment around the central axis of the corrugated slab is estimated from the relation

$$I_2 = \frac{L}{2} r_e^2 t \tag{1}$$

The inertial moment of the longitudinal cross-section of the wall around the central horizontal axis of the simple tube is given by

$$I_1 = \frac{Lt^3}{12} \tag{2}$$

From equations (1) and (2), the ratio of the inertia moment of the corrugated tube to the inertia moment of the simple tube is obtained as

$$\frac{\mathrm{I}_2}{\mathrm{I}_1} = 6\left(\frac{r_e}{t}\right)^2 \tag{3}$$

According to the above relation, the strength of the curved plate of the specimen wall against the local bending deformation at the plastic hinge lines is

Table 1. Geometrical characteristics, masses and shapes of the empty specimens for the lateral flattening tests.

Specimen code	R_i (mm)	t (mm)	L (mm)	m (g)	r_e (mm)	Shape
LE-28	22	0.5	27.3	39.89	9.5	CCT
LE-29	35.9	0.4	78	76.98	7.7	PCT
LE-30	27.3	0.5	27	38.81	10.2	CCT
LE-31	35.9	0.5	30	80.43	12	CCT
LE-32	22	0.4	57.3	37.08	6.4	PCT
LE-33	27.3	0.4	66	25.24	7.65	PCT
LE-34	27.3	0.5	64.8	47.05	7.5	PCT
LE-35	27.3	0.6	61.2	58.44	5.5	PCT
LE-36	35.9	0.5	83.4	75.92	5.8	PCT
LE-38	35.9	0.6	56	57.64	—	CT
LE-39	35.9	0.5	57	45.5	—	CT
LE-40	35.9	0.4	58	36.11	—	CT
LE-42	27.3	0.5	46.5	27.67	—	CT
LE-44	22	0.4	47	18.73	—	CT
LE-45	55.4	0.5	77.5	95.72	—	CT
LE-46	55.4	0.6	114	176.92	5	PCT
LE-47	55.4	0.5	107.4	143.01	8.5	PCT
LE-48	55.4	0.7	82.5	135.8	—	CT
LE-49	55.4	0.6	77.5	118.91	—	CT
LE-50	55.4	0.7	92.4	157.53	8.5	PCT
LE-54	55.4	0.5	34.5	174.92	14	CCT

CCT: complete corrugated tube; PCT: preformed corrugated tube; CT: circular tube.

Table 2. Geometrical characteristics, masses and shapes of the foam-filled specimens for the lateral flattening tests.

Specimen code	R_i (mm)	t (mm)	L (mm)	m (g)	r_e (mm)	Shape
LF-82	22	0.5	18.2	27.5	9.5	CCT
LF-83	35.9	0.4	51	70.29	7.7	PCT
LF-84	27.3	0.5	18	27.17	10.2	CCT
LF-85	35.9	0.5	20	58.70	12	CCT
LF-86	22	0.4	38.2	29.13	6.4	PCT
LF-87	27.3	0.4	44	32.22	7.65	PCT
LF-88	27.3	0.6	40.8	43.9	5.5	PCT
LF-89	35.9	0.5	55.6	69.12	5.8	PCT
LF-92	35.9	0.5	57	60.45	—	CT
LF-93	35.9	0.4	58	52.08	—	CT
LF-94	27.3	0.6	48	42.01	—	CT
LF-95	27.3	0.5	46.5	33.08	—	CT
LF-96	27.3	0.4	51	29.55	—	CT
LF-97	22	0.4	47	21.99	—	CT
LF-98	55.4	0.5	77.5	131.52	—	CT
LF-99	55.4	0.7	82.5	177.55	—	CT
LF-101	55.4	0.7	61.6	144.92	8.5	PCT
LF-102	55.4	0.6	76	161.76	5	PCT
LF-103	55.4	0.5	71.6	143.74	8.5	PCT
LF-104	27.3	0.5	43.2	36.79	7.5	PCT
LF-105	55.4	0.5	23	119.75	14	CCT

CCT: complete corrugated tube; PCT: preformed corrugated tube; CT: circular tube.

dependent on the second power of the r_e/t ratio. Therefore, by increasing the corrugation radius of the corrugated tubes during the hydroforming process, the energy absorbed by the corrugated tubes increases markedly.

Figure 6 shows the experimental diagrams of the absorbed energy per unit of specimen mass versus the lateral displacement of the specimens recorded in Figure 4. The curves were drawn by calculating the area under the corresponding load versus displacement diagram. The ratio of the absorbed energy to the mass indicates the specific absorbed energy. According to Figure 6(a), it is found that the empty complete corrugated tube has the highest specific absorbed energy, in comparison with those of the corresponding empty circular tube and the preformed corrugated tube. As a numerical study, the experimental measurements show that, up to the same lateral displacement of 100.62 mm, the absorbed-energy-to-mass ratios of the empty circular tube, the preformed corrugated tube and the

Table 3. Geometrical characteristics, masses and shapes of the empty specimens for the axial folding tests.

Specimen code	R_i (mm)	t (mm)	L (mm)	m (g)	r_e (mm)	Shape
AE-1	22	0.5	27.3	39.89	9.5	CCT
AE-2	35.9	0.4	78	79.21	7.7	PCT
AE-3	27.3	0.5	64.8	47.06	7.5	PCT
AE-6	55.4	0.5	34.5	174.03	14	CCT
AE-7	27.3	0.5	27	38.18	10.2	CCT
AE-8	55.4	0.7	92.4	159.63	8.5	PCT
AE-9	22	0.4	57.3	36.87	6.4	PCT
AE-10	27.3	0.6	61.2	57.34	5.5	PCT
AE-12	27.3	0.5	85	53.46	—	CT
AE-13	27.3	0.4	80	46.03	—	CT
AE-14	22	0.4	84	35.04	—	CT
AE-15	35.9	0.5	110	94.21	—	CT
AE-17	35.9	0.4	108	74.98	—	CT
AE-18	55.4	0.7	129	249.66	—	CT
AE-19	55.4	0.5	134	173.6	—	CT
AE-21	55.4	0.6	134	215.75	—	CT
AE-22	27.3	0.4	66	38.17	7.65	PCT
AE-23	35.9	0.5	30	76.96	12	CCT
AE-24	35.9	0.5	83.4	79.93	5.8	PCT

CCT: complete corrugated tube; PCT: preformed corrugated tube; CT: circular tube.

Table 4. Geometrical characteristics, masses and shapes of the foam-filled specimens for the axial folding tests.

Specimen code	R_i (mm)	t (mm)	L (mm)	m (g)	r_e (mm)	Shape
AF-55	22	0.5	18.2	27.22	9.5	CCT
AF-56	35.9	0.4	51	67.53	7.7	PCT
AF-58	27.3	0.5	43.2	40.76	7.5	PCT
AF-61	55.4	0.5	23	123.28	14	CCT
AF-62	27.3	0.5	18	30.11	10.2	CCT
AF-63	55.4	0.7	61.6	138.03	8.5	PCT
AF-64	22	0.4	38.2	28.64	6.4	PCT
AF-65	27.3	0.6	40.8	43.70	5.5	PCT
AF-66	27.3	0.6	83	81.2	—	CT
AF-67	27.3	0.5	85	68.02	—	CT
AF-68	27.3	0.4	80	55.14	—	CT
AF-69	22	0.4	84	37.14	—	CT
AF-70	35.9	0.5	110	95.97	—	CT
AF-71	35.9	0.6	110	120.37	—	CT
AF-72	35.9	0.4	108	76.32	—	CT
AF-75	27.3	0.4	44	24.67	7.65	PCT
AF-76	35.9	0.5	20	53.67	12	CCT
AF-77	55.4	0.6	134	220.18	—	CT

CCT: complete corrugated tube; PCT: preformed corrugated tube; CT: circular tube.

complete corrugated tube are 329 J/kg, 1627 J/kg and 4266 J/kg respectively. The results show that the specific absorbed energy of the empty complete corrugated tube is 12.97 times the specific absorbed energy of the corresponding circular tube. Also, the specific absorbed energy of the empty preformed corrugated tube is 4.94 times the corresponding value of the circular tube. The specific absorbed energy is the most important parameter in the design of an energy absorber to improve the safety of some systems such as automotive systems. The results show that, by shaping the circular tube into a corrugated tube by the hydroforming process, a new structure with a very higher energy absorption capability is gained. This shows the considerable advantage of using a complete corrugated tube as an energy absorber instead of a circular tube, in the flattening loading condition.

In the foam-filled condition, the complete corrugated tube LF-85, the preformed corrugated tube LF-89 and the simple circular tube LF-92 are compared. The specific absorbed energies of these specimens are 2628 J/kg, 2370 J/kg and 1869 J/kg respectively. The compared results show that the order of the foam-filled specimens is as same as that of the empty specimens. This means that the complete corrugated tube has the highest specific absorbed energy in comparison with the other specimens. Also, the specific absorbed energy of the preformed corrugated tube is higher than that of

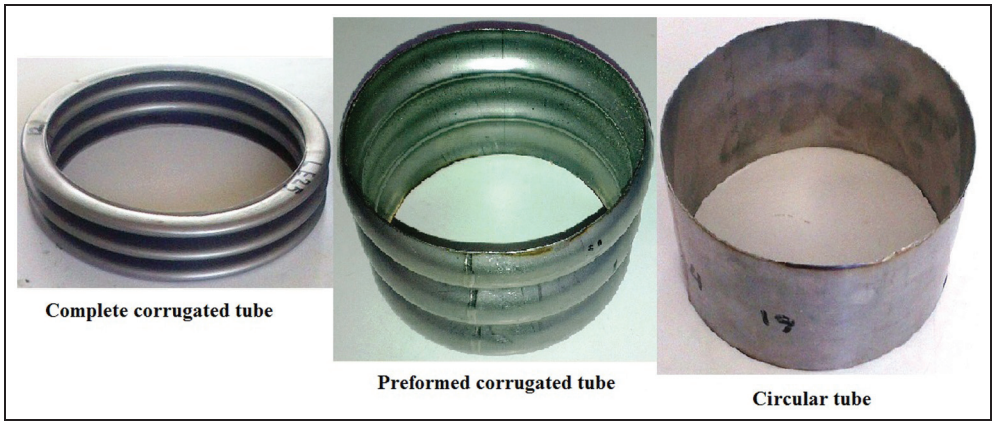

Figure 1. Three different geometrical types of empty specimen before the tests.

Figure 2. Foam-filled steel E304 tubes of three different geometrical types before the tests.

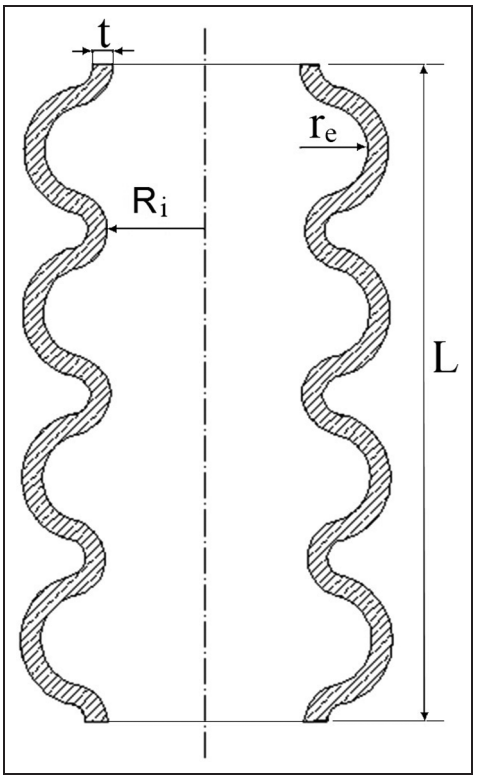

Figure 3. Schematic shapes of the corrugated specimens.

the corresponding simple tube. The specific absorbed energy of the complete corrugated tube is 1.41 times the specific absorbed energy of the corresponding circular tube. Also, the specific absorbed energy of the preformed corrugated tube is 1.27 times the corresponding value of the circular tube.

In Figure 4(b), a sudden decrease appeared in the applied lateral load on the filled specimen LF-85. Experimental observations show that a sudden lateral buckling occurred in the filled specimen LF-85. When a circular tube is shaped into a complete corrugated tube, the strength of the specimen against the lateral compression considerably increases, according to equation (2). Also, the presence of polyurethane foam filler enhances the lateral load. Therefore, filling a complete corrugated tube by foam causes a considerable increase in the lateral load of the flattening process, with respect to the corresponding simple circular tube in the empty condition. Also, the required load for the lateral flattening of the complete corrugated tube may become higher than the required load for lateral buckling of the specimen. This was the reason for the sudden decrease in the corresponding curve for specimen LF-85 in Figure 4(b).

Effect of the diameter. Figure 7(a) compares the experimental load-to-mass ratio versus displacement diagrams of the flattening tests on specimens LE-28, LE-30, LE-31 and LE-54. These specimens are empty complete corrugated tubes, and they have the same wall

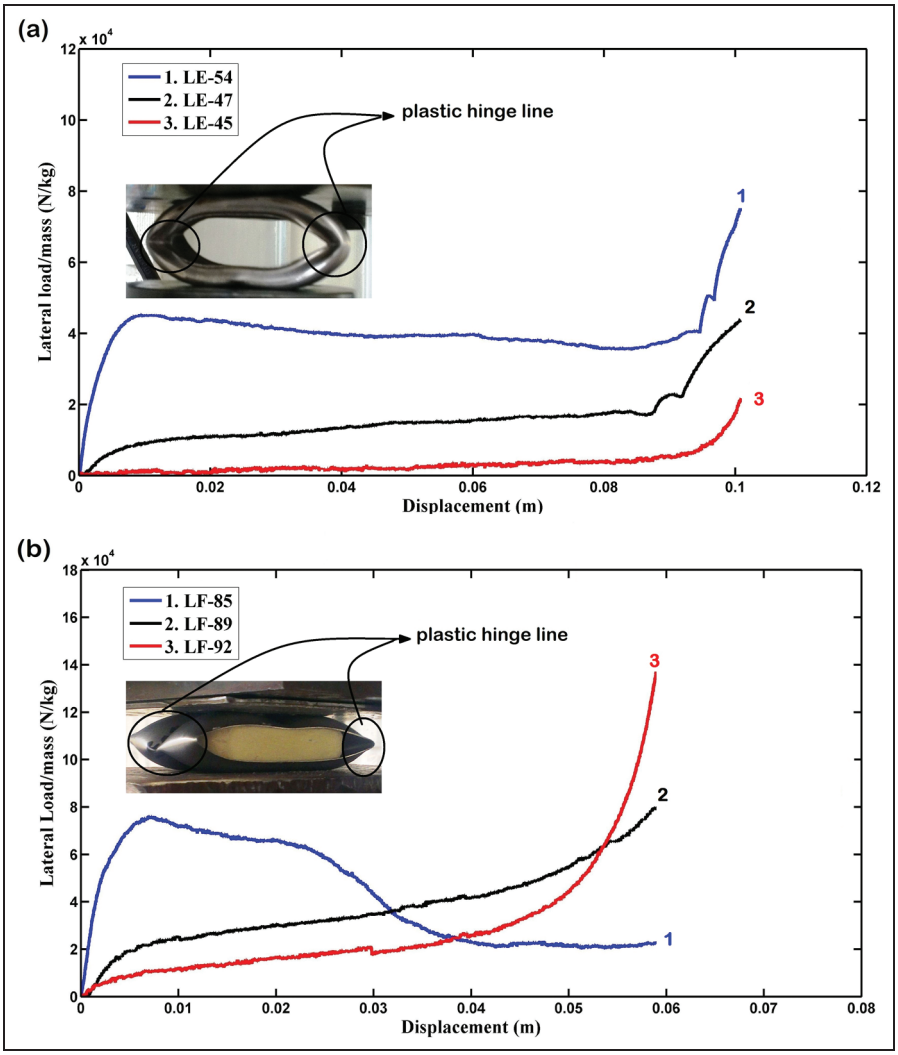

Figure 4. Lateral-load-to-mass ratio versus lateral displacement curves of circular tubes, preformed corrugated tubes and complete corrugated tubes: (a) empty specimens; (b) foam-filled specimens.

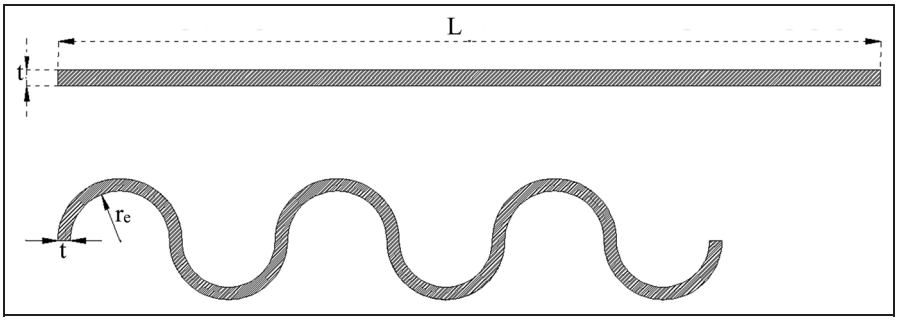

Figure 5. Two slabs showing the longitudinal cross-sections of the simple tube and the corrugated specimen.

thicknesses and the same material properties, but with different diameters. Figure 7(b) shows the corresponding curves for specimens LF-82, LF-84, LF-85 and LF-105 in the polyurethane-foam-filled condition. Figure 7(b) shows that, at a certain displacement, the lateral loads of the specimens with smaller diameters are higher than those of the the specimens with larger diameters. However, at the end of the lateral compression process, the lateral displacements of specimens with smaller diameters are less than those of specimens with larger diameters. Therefore, for both empty corrugated tubes and filled complete corrugated tubes, by increasing the diameter, the lateral compressive load is reduced, while the final crushing course increased.

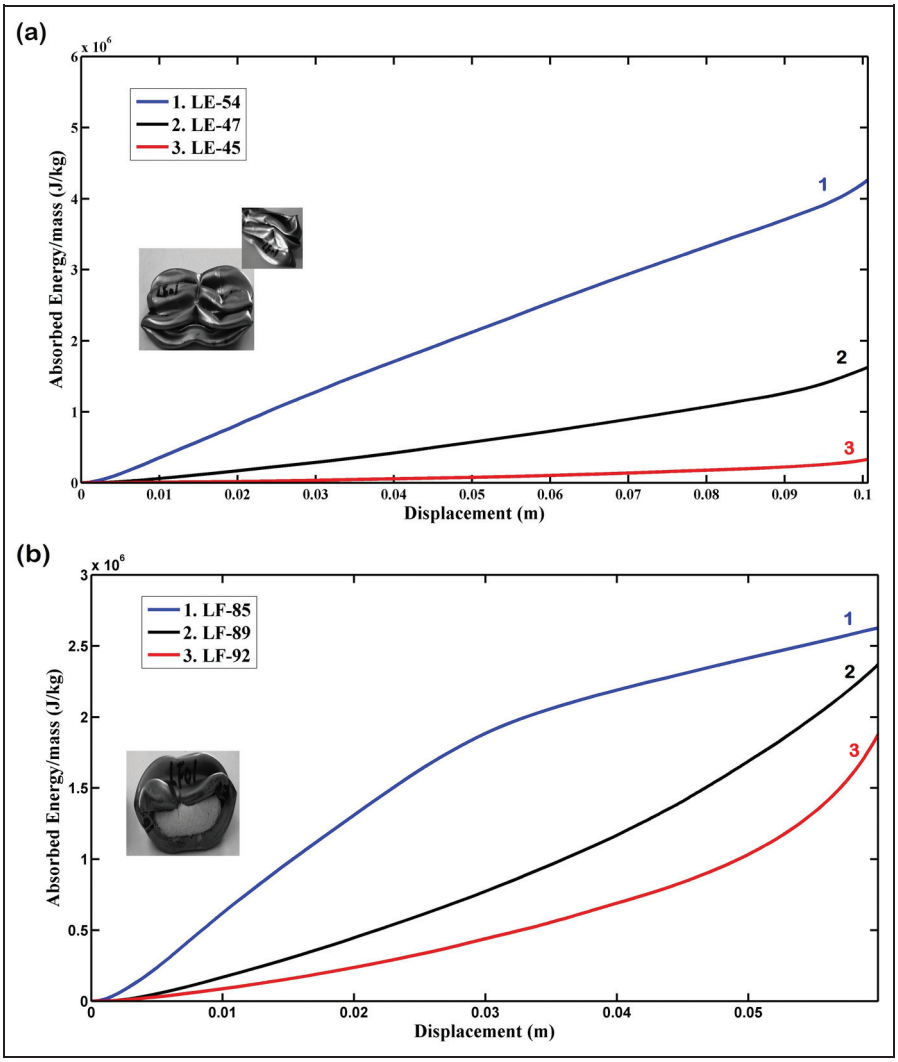

Figure 6. Absorbed-energy-to-mass ratio versus lateral displacement curves of circular tubes, preformed corrugated tubes and complete corrugated tubes with different diameters: (a) empty specimens; (b) foam-filled specimens.

In the design of an ideal energy absorber system, one of the main parameters is the crushing force efficiency (CFE), and it is defined as the ratio of the mean load to the initial peak load. The CFE of an ideal energy absorber is equal to 1. As a numerical investigation, the CFEs of the polyurethane-foam-filled complete corrugated tubes LF-82, LF-84, LF-85 and LF-105 are obtained as 0.735, 0.687, 0.562 and 0.721 respectively. The results show that, from the viewpoint of the CFE, there are some optimum diameters for foam-filled complete corrugated tubes, and the filled specimens with initial inner radii of 55.4 mm and 22.0 mm have CFEs higher than 70%. Also, the experimental measurements show that the CFEs of the empty specimens LE-28, LE-30, LE-31 and LE-54 are 0.851, 0.733, 0.873 and 0.925 respectively. This means that, on the basis of the CFE, for empty complete corrugated tubes, there are several optimum diameters, and the empty complete corrugated tube with an initial inner radius of 55.4 mm has a CFE higher than 90% and the empty specimens with initial inner radii of 35.9 mm and 22 mm have CFEs higher than 80%. Totally, the results show that in both the empty conditions and the filled conditions of complete corrugated tubes, the specimen with the smallest radius of 22 mm and also the specimen with the largest radius of 55.4 mm have CFEs higher than 0.7, which are both acceptable results.

Figure 8 illustrates the experimental diagrams of the absorbed energy per unit of mass versus lateral displacement of the empty specimens with different conditions. Figure 8(a) compares the results of the empty complete corrugated tubes LE-28, LE-30, LE-31 and LE-54 which have the same wall thicknesses and the same material types, but different diameters. According to Figure 8(a), for the empty complete corrugated tubes, when the diameter of the specimen increases, the specific absorbed energy of the specimen decreases. This means that a complete corrugated tube with a smaller diameter is a better energy absorption system, in comparison with a similar specimen with a larger diameter. Comparison of the results shows that the diameter of specimen LE-28 is 38.2% less than the

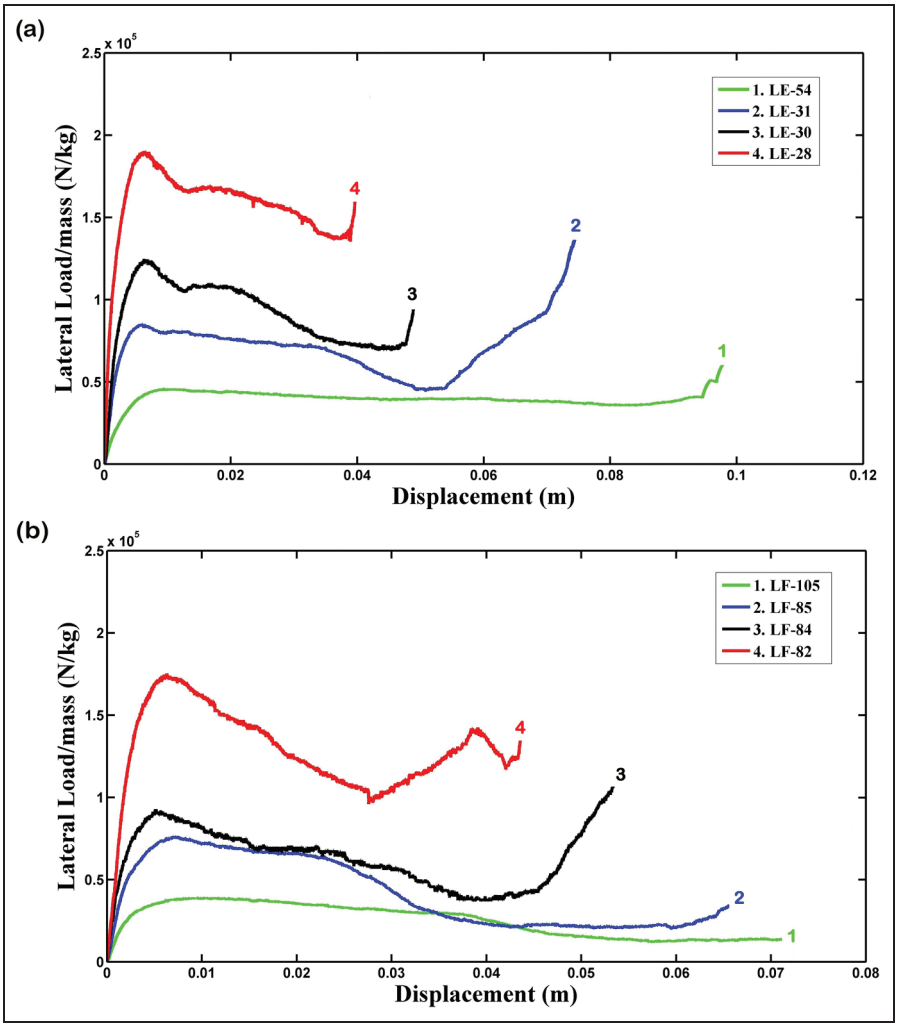

Figure 7. Lateral-load-to-mass ratio versus displacement diagrams of complete corrugated tubes with different diameters: (a) empty specimens; (b) foam-filled specimens.

diameter of specimen LE-31, while the total absorbed energy of specimen LE-28 is 1.83 times the corresponding value of specimen LE-31.

An experimental comparison between the absorbed-energy-to-mass ratio versus displacement diagrams of the empty preformed corrugated tubes LE-34, LE-36 and LE-47 is given in Figure 8(b). The specimens have the same material types and wall thicknesses, but different diameters. Figure 8(b) shows that, up to a certain displacement, the absorbed energy of specimens with smaller diameters is higher than those of the other specimens but, at the end of the flattening process on empty preformed corrugated tubes with different diameters, the specific absorbed energies of the different specimens are approximately the same. For empty preformed corrugated tubes, the specimens with larger diameters have less lateral load during the process owing to the longer bending moment arm around the two plastic hinge lines; also, they have higher lateral displacements at the end of the process. Therefore, by increasing and also by decreasing the diameter, the total absorbed energies of empty preformed corrugated specimens may remain constant. Figure 9 illustrates the bending moment arm in a filled specimen.

Figure 8(c) compares the absorbed energy-to-mass ratio versus displacement curves of the simple circular tubes LE-45, LE-39 and LE-42 with the same wall thicknesses and the same material properties, but with different diameters. The experimental results in Figure 8(c) show that, when the diameter of the circular tubes increases, the specific absorbed energy of the specimen decreases. Therefore, it is found that a circular tube with a smaller diameter is a better energy absorber.

Figure 10 shows the diagrams of the absorbed energy-to-mass ratio versus the compressive displacement of the corresponding polyurethane-foam-filled specimens with different initial diameters. The specimens in Figure 10(a) are filled complete corrugated tubes, the specimens in Figure 10(b) are filled preformed corrugated tubes and the specimens in Figure 10(c) are filled simple circular tubes. Figure 10(a) and (b) indicates that, when the strength-to-weight ratio of filled corrugated specimens obtained by the hydroforming method is the main parameter of design, specimens

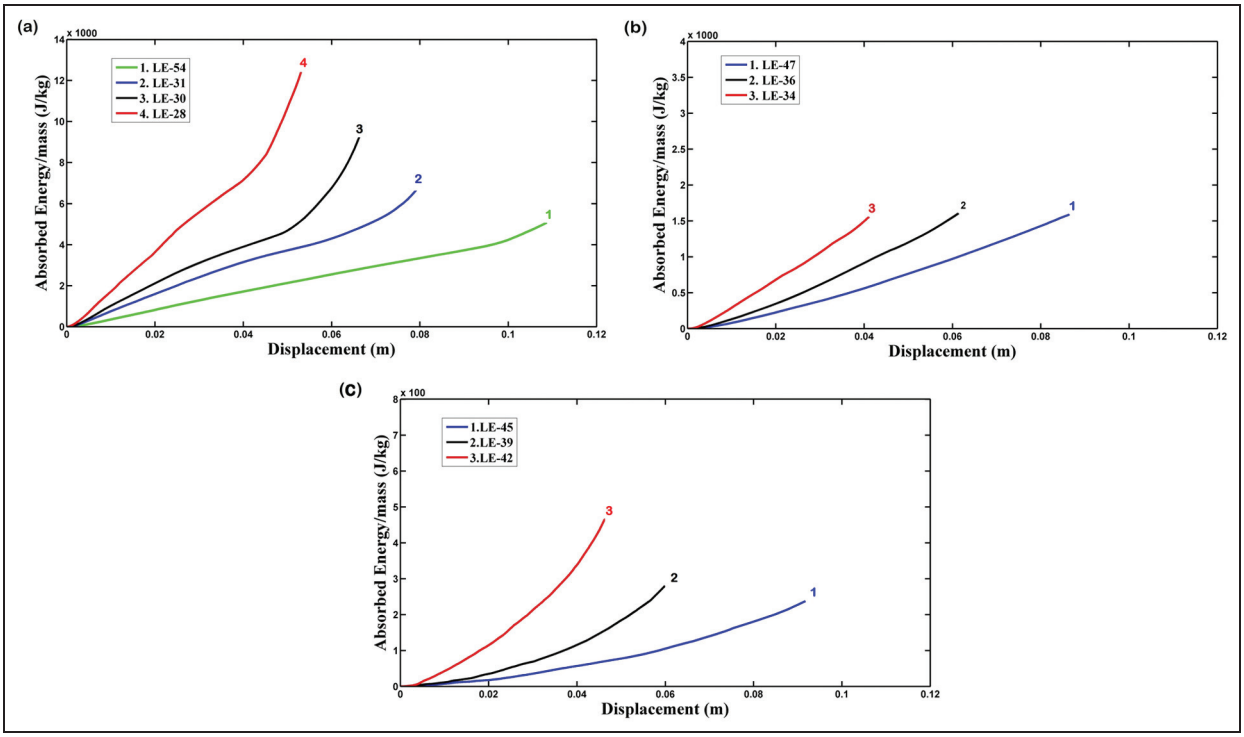

Figure 8. Absorbed-energy-to-mass ratio versus displacement diagrams of empty specimens with different diameters: (a) complete corrugated tubes; (b) preformed corrugated tubes; (c) simple circular tubes.

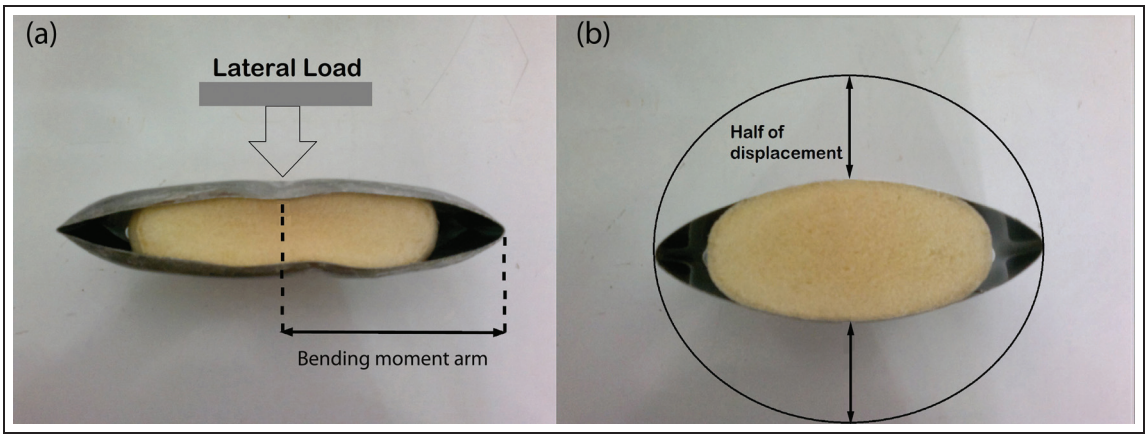

Figure 9. (a) Bending moment arm in a filled preformed corrugated tube; (b) lateral displacement in a polyurethane-foam-filled simple circular tube.

with smaller diameters are a more desirable selection. From another viewpoint, according to Figure 7(b), by enhancing the diameters of filled corrugated tubes, the lateral load decreases; therefore, the applied load on the other parts of the structure decreases, which is a considerable factor in the design of some cases. In this scenario, it is suggested that it is better to select a filled corrugated tube with a larger diameter.

According to Figure 10(c) which compares the absorbed-energy-to-mass ratio versus displacement curves of polyurethane-foam-filled simple circular tubes with different diameters, it is found that a tube with a larger diameter has a better performance.

Generally, on the basis of the studied experiments and the investigated cases, it is concluded that, when the principal design factor is the strength-to-weight ratio, a flattened energy absorber with a corrugated shape and with a smaller diameter is a better choice but, if the transmitted load to different components of a structure has the key role, it is prefereable to select a corrugated energy absorber with an optimized diameter.

Effect of the wall thickness. Figure 11 shows the absorbed-energy-to-mass ratio versus displacement diagrams of

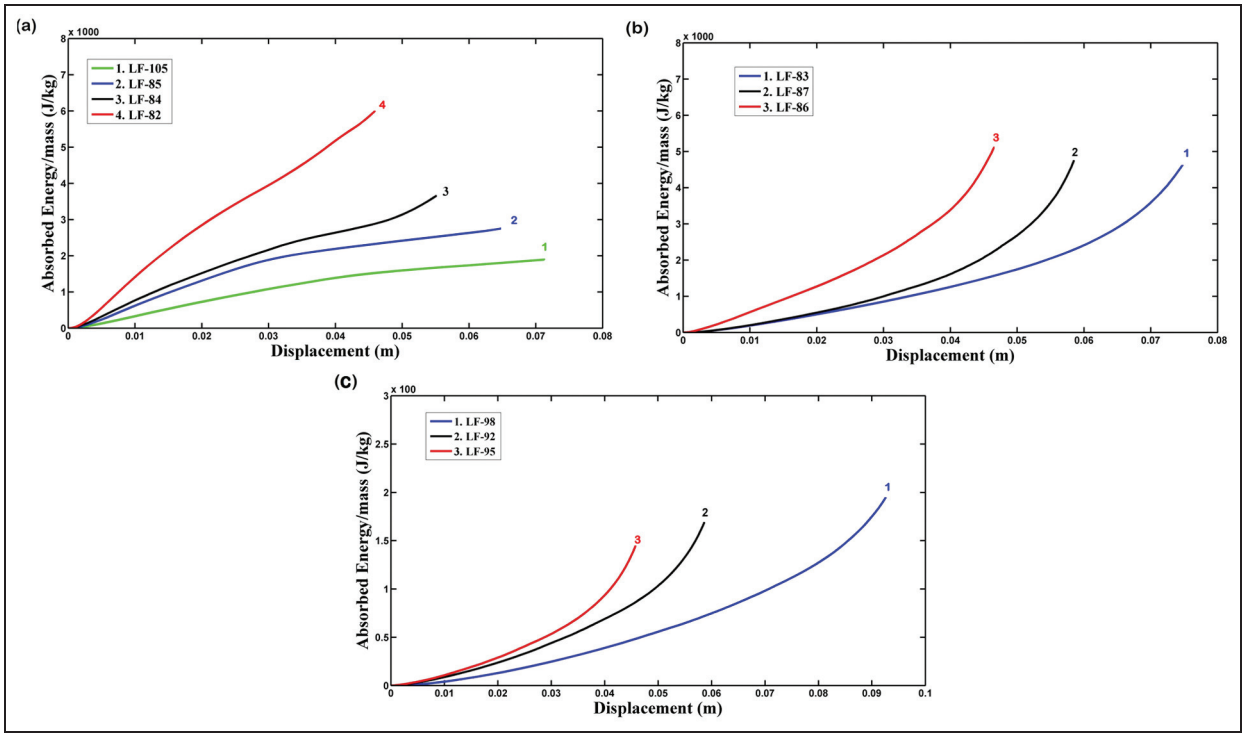

Figure 10. Absorbed-energy-to-mass ratio versus displacement diagrams of foam-filled specimens with different diameters: (a) complete corrugated tubes; (b) preformed corrugated tubes; (c) simple circular tubes.

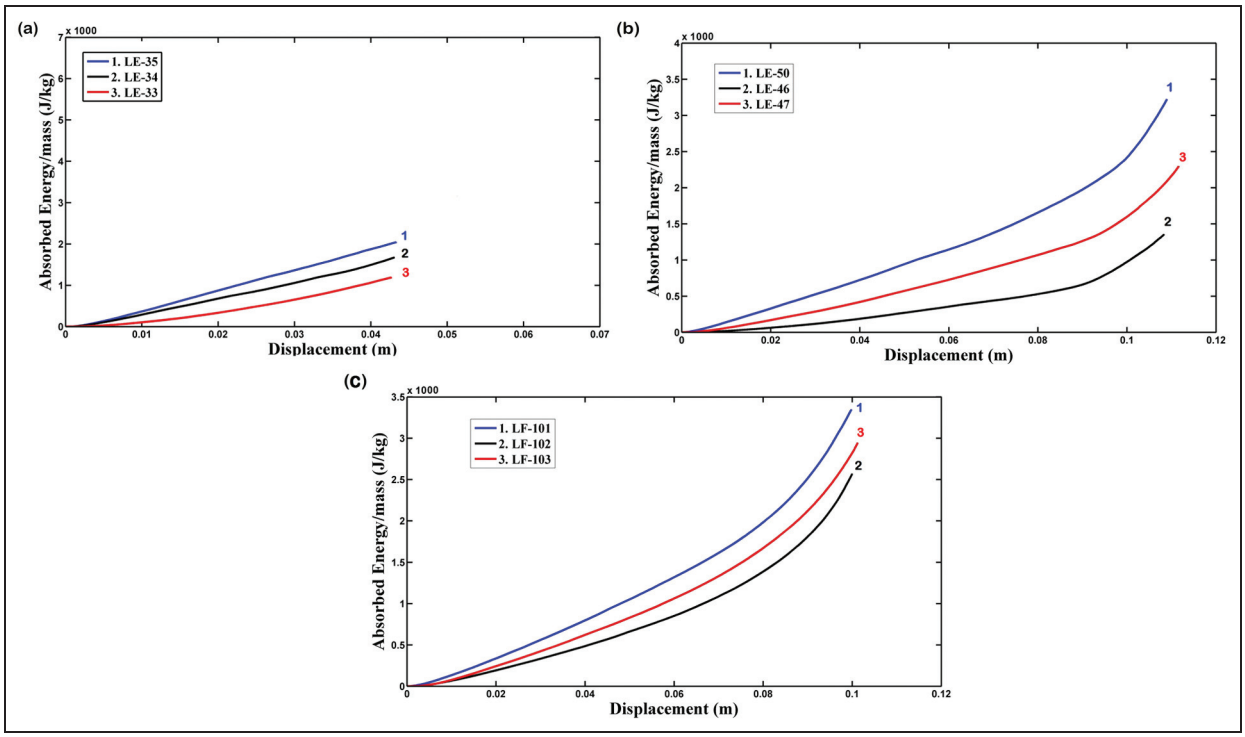

Figure 11. Absorbed-energy-to-mass ratio versus displacement diagrams of preformed corrugated tubes with different wall thicknesses: (a) empty, R_i = 27.3 mm; (b) empty, R_i = 55.4 mm; (c) foam filled, R_i = 55.4 mm.

preformed corrugated tubes with the same material types and diameters, but with different wall thicknesses. Figure 11(a) shows the curves of empty corrugated specimens with an inner radius of 27.3 mm. Comparison of the curves indicates that for empty preformed corrugated tubes, by increasing the wall thickness, the specific absorbed energy also increases. Figure 11(b) illustrates the corresponding curves of the empty

preformed corrugated tubes with an inner radius of 55.4 mm. There is an interesting result in this figure. Figure 11(b) shows the curves of empty preformed corrugated specimens LE-50, LE-46 and LE-47 with wall thicknesses of 0.7 mm, 0.6 mm and 0.5 mm respectively and corrugation radii of 8.5 mm, 5.0 mm and 8.5 mm respectively and demonstrates that, although the wall thickness of specimen LE-47 is less than that of specimen LE-46 and the corrugation radii of specimen LE-47 are larger than those of specimen LE-46, the specific absorbed energy of specimen LE-47 is 1.62 times the corresponding value of specimen LE-46. It shows that the corrugation shaping of tubes has a considerable effect on the total absorbed energy of the structures, in comparison with that of the corresponding simple tube.

Figure 11(c) gives an experimental comparison of the absorbed-energy-to-mass ratios versus displacement diagrams of the preformed corrugated tubes LF-101, LF-102 and LF-103 in the filled condition. The material types and the corrugation radii of specimens LF-101 and LF-103 are the same, but specimen LF-101 is a thicker specimen. The curves show that the specific absorbed energy of the thicker specimen LF-101 is 20% higher than that of specimen LF-103; however, its wall is 40% thicker than that of the corresponding specimen LF-103. Therefore, in the investigated corrugated tubes with a polyurethane foam filler, by increasing the wall thickness of the tube, the specific absorbed energy is enhanced. Also, in Figure 11(c), the wall thickness of specimen LF-102 is larger than that of specimen LF-103, but the corrugation radius of specimen LF-102 is less than that of specimen LF-103. The specific absorbed energies of specimen LF-102 and specimen LF-103 are 2653 J/kg and 2912 J/kg respectively. Thus, the specific absorbed energy of specimen LF-103 is 10% higher than that of specimen LF-102. This shows that the corrugation radius of a corrugated tube has a considerable effect on the specific absorbed energy of the specimen. In other words, during the shaping process of a circular tube into a corrugated tube by the hydroforming method, a structure with a higher energy absorption capability is gained.

Experimental diagrams of the absorbed-energy-to-mass ratio versus the displacement of simple circular tubes with the same material types and same diameters, but with different wall thicknesses are drawn in Figure 12. Figure 12(a) and (b) show the curves of empty specimens with inner radii of 35.9 mm and 55.4 mm respectively. Also, Figure 12(c) illustrates the corresponding diagram for foam-filled simple tubes with an inner radius of 27.3 mm. It is found that, for the studied cases in Figure 12(a) with an inner radius of 35.9 mm, thicker empty simple tubes absorb a higher energy per unit of mass. However, the curves in Figure 12(b) for empty simple tubes with an inner radius of 55.4 mm show that, in this case, there is an optimum value for the wall thickness of the tube, and an empty simple specimen with the optimum thickness has the highest specific absorbed energy. Previously, Niknejad et al.[19] investigated the flattening process of simple circular tubes, but they did not investigate the effects of the wall thickness of empty tubes, obviously. The results of the present work show that in empty simple tubes, depending on the tube diameter, there is an optimum wall thickness, based on the specific absorbed energy. Therefore, in empty simple tubes, the value of the wall thickness has a considerable effect on the energy absorption capability.

According to the curves of filled circular tubes in Figure 12(c), it is found that, by increasing the wall thickness, although the energy absorption capability of the specimens increases, the mass of the structure also increases. Since the rate of increase in the mass is larger than the rate of increase in the absorbed energy of polyurethane-foam-filled tubes, the specific absorbed energies of simple tubes with thinner walls are higher than those with thicker walls. This means that, for filled simple tubes, the presence of light polyurethane foam filler has a greater share of the total absorbed energy than the wall thickness of the tube does.

Effect of the foam filler. Figure 13 compares the specific absorbed energy of the empty specimens and the corresponding polyurethane-foam-filled specimens during the crushing process. This figure shows that, for the simple tube specimens, the specific absorbed energies of the filled circular tube LF-98 and the corresponding empty tube LE-45 are 1750 J/kg and 222 J/kg respectively. Thus, the specific absorbed energy of the filled specimen with an initial radius of 55.4 mm is 7.87 times the specific absorbed energy of the similar empty specimen. Also, according to the experimental measurements, it is found that, for simple tubes with an initial radius of 22 mm, the specific absorbed energy of the filled specimen LF-97 is 2.96 times the specific absorbed energy of the similar empty tube. Thus, it is understood that filling a simple circular tube with polyurethane foam increases the ratio of the total absorbed energy to the mass of a structure considerably. Also, by increasing the tube diameter, the advantage of a foam-filled specimen over an empty specimen increases. This is due to the higher volume of polyurethane foam filler in a tube with a larger diameter. Therefore, for a filled tube with the initial simple form, the polyurethane foam filler has a higher share of total absorbed energy, in comparison with that of the tube. On the other hand, for simple circular tubes, a filled specimen is a better energy absorber than the corresponding empty tube.

Figure 13 also illustrates the specific absorbed energies of preformed corrugated tubes in two different conditions: empty and foam filled. In each pair of mentioned specimens in the figure, one specimen is empty and the other is foam filled, with the same geometrical characteristics and same material properties. The empty preformed corrugated tube LE-29 and the corresponding filled tube LF-83 with the same initial radius of 35.9 mm have specific absorbed energies of 4121 J/kg

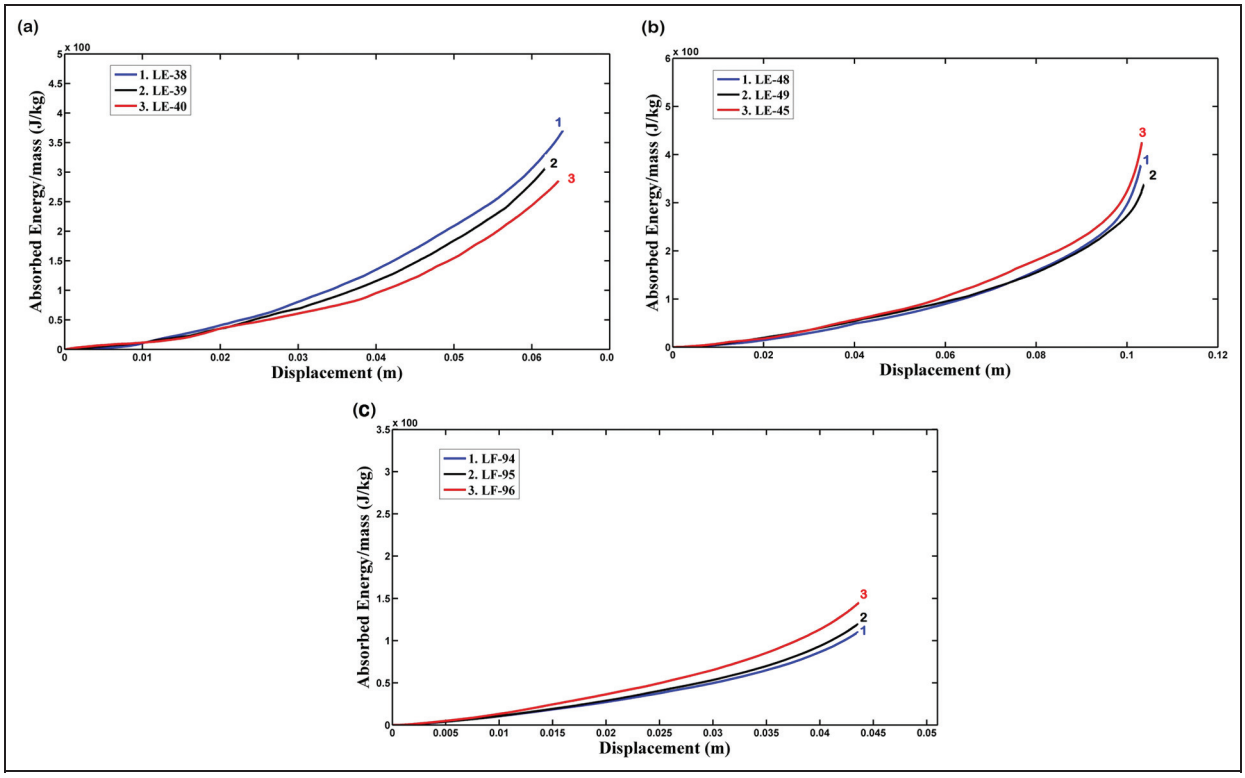

Figure 12. Absorbed-energy-to-mass ratio versus displacement diagrams of circular tubes with different wall thicknesses: (a) empty, R_i = 35.9 mm; (b) empty, R_i = 55.4 mm; (c) foam filled, R_i = 27.3 mm.

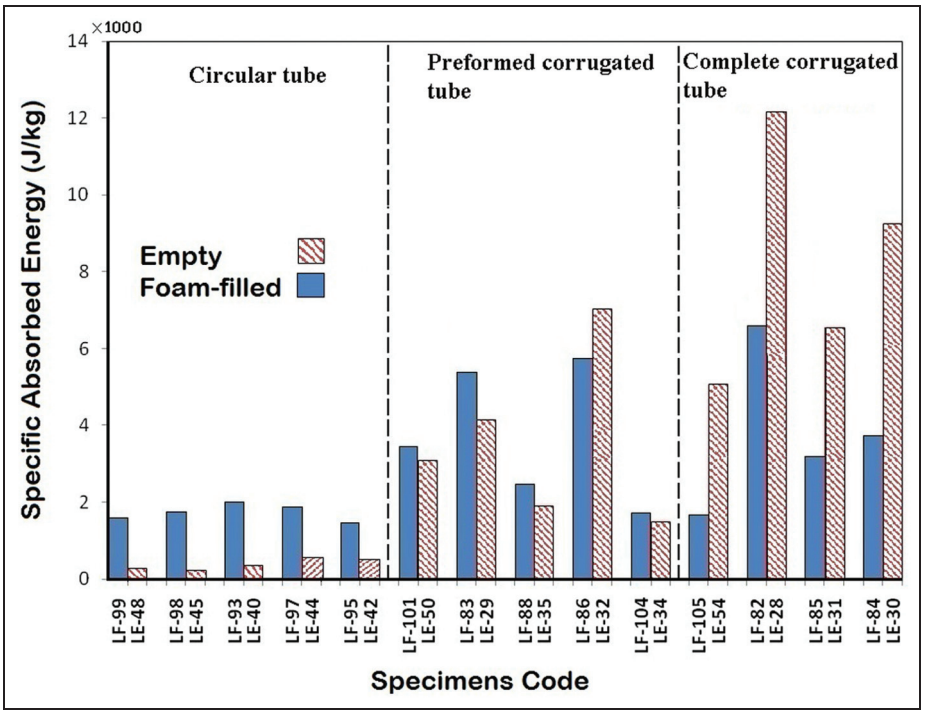

Figure 13. Comparison of the specific absorbed energies of empty specimens and corresponding polyurethane-foam-filled specimens during lateral compression.

and 4829 J/kg respectively. This shows that the specific absorbed energy of the filled preformed specimen is 1.18 times the specific absorbed energy of the corresponding empty specimen. Also, the results indicate that the ratio of the specific absorbed energy of the filled preformed specimen to that of the empty preformed specimen with an initial radius of 27.3 mm is 1.06 and the corresponding ratio for preformed

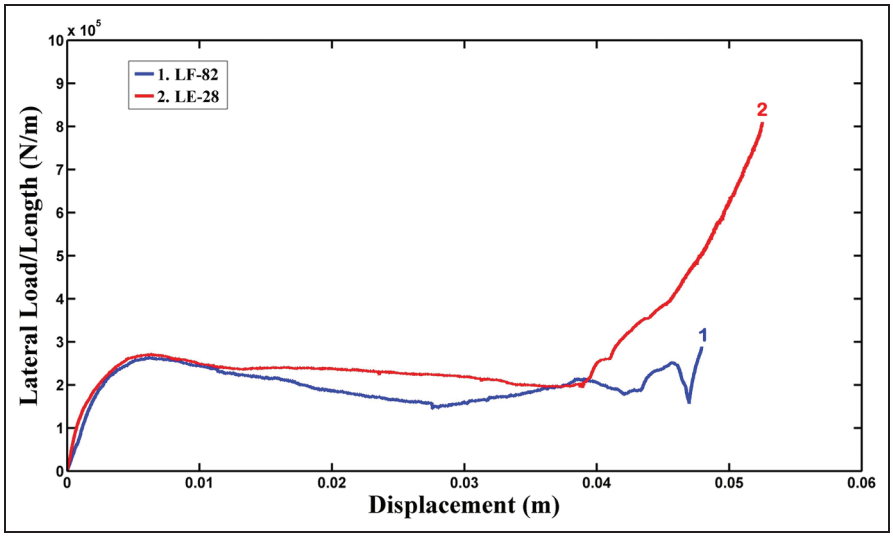

Figure 14. Lateral-load-to-length ratio versus displacement curves of the complete corrugated tubes LE-28 and LF-82 with different filling conditions.

specimens with an initial radius of 22 mm is equal to 0.82. The obtained comparisons show that, for the preformed corrugated tubes, the total absorbed energy per unit of mass of the filled specimen is almost the same as that of the similar empty specimen. Furthermore, for preformed specimens with larger diameters, the polyurethane foam as the filler has a positive impact on the crushing behaviour of the structure, but this effect is insignificant in comparison with that for simple circular tubes. Reviewing the results shows that the ratio of the specific absorbed energy of the foam-filled preformed specimen to that of the empty preformed specimen has a range 0.82–1.18 and the ratio changes owing to the different wall thicknesses and the different diameters of the specimens. This means that, for preformed corrugated tubes, filling the specimens which have larger diameters with polyurethane foam has a smooth positive effect on the energy absorption behaviour of the structure, and it has a negative effect on specimens which have smaller diameters. Therefore, for filled preformed corrugated tubes, a considerable share of the total dissipated energy is absorbed by the tube alone.

An experimental comparison between the lateral-load-to-length ratio versus displacement curves of the complete corrugated tubes LE-28 and LF-82 with different filling conditions (empty and polyurethane foam filled) but with other characteristics which are the same are given in Figure 14; this shows an unpredicted result. At a certain displacement of lateral compression, the polyurethane foam becomes like a rigid material without any void, and so the ultimate lateral displacement of the filled specimen is less than that of the empty specimen. However, even up to the same displacement, the absorbed energy of the empty complete corrugated tube is higher than that of the corresponding filled tube. Figure 14 shows that, at the commencement of the flattening process on the empty complete corrugated tube, two plastic hinge lines are created at the left side and the right side of the specimen. During the compression, the corrugated wall of the empty complete corrugated tube at the plastic hinge lines is shaped into a flat wall. Therefore, according to equation (2), a high lateral load is required to flatten the empty tube but, in the foam-filled complete corrugated tube, the polyurethane foam filler prevents the creation of plastic hinge lines at the left side and the right side of the specimen, at the commencement of the test. Therefore, the curve of the lateral-load-to-length ratio versus displacement of the filled specimen is lower than that of the empty specimen. Also, for the filled specimen, after a certain displacement, because of the rigidity of the polyurethane foam, the maximum compressive displacement is less than that of the corresponding empty specimen. This means that, for filled complete corrugated tubes, the corrugated wall of the specimen does not suffer a considerable change. Therefore, the polyurethane foam filler changes the deformation mode of complete corrugated tubes during the flattening process and it results in lower energy absorption capacities of filled specimens than those of similar empty specimens.

In order to reach a better conclusion, the specific absorbed energies of foam-filled complete corrugated tubes and the corresponding empty specimens are compared in Figure 13 to study the effect of the polyurethane foam filler on the flattening process of the complete corrugated tubes. The numerical results indicate that the specific absorbed energies of the empty specimen LE-28 and the filled specimen LF-82 are 12,138 J/kg and 6022 J/kg respectively. This means that, for complete corrugated tubes with an initial radius of 22 mm, the specific absorbed energy of the filled specimen 50.38% decreases owing to the filler. These reductions for specimens with initial radii of 27.3

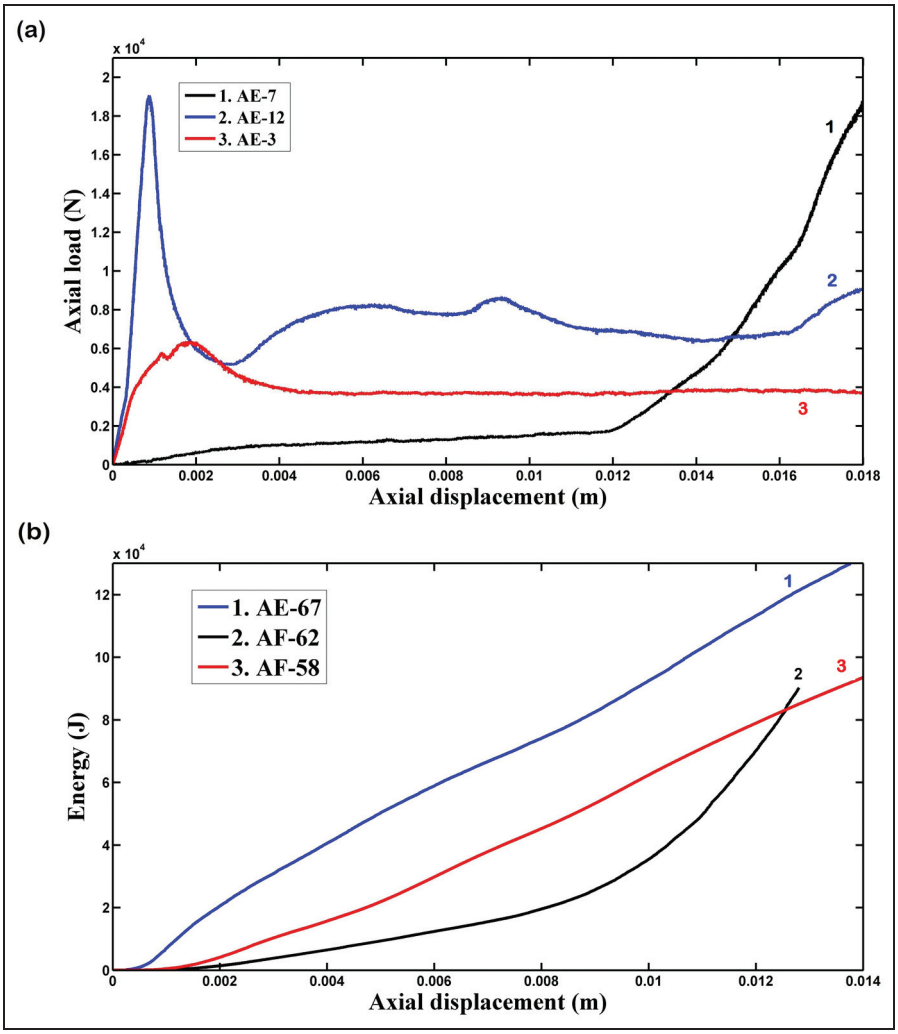

Figure 15. (a) Axial load versus displacement curves of the empty circular tube, the preformed corrugated tube and the complete corrugated tube; (b) absorbed energy versus axial displacement curves of the foam-filled circular tube, the foam-filled preformed corrugated tube and the foam-filled complete corrugated tube.

mm, 35.9 mm and 55.4 mm are 59.6%, 59.6% and 66.9% respectively. Therefore, for complete corrugated tubes, specimens in the empty condition are better energy absorbers than the corresponding filled specimens are.

More comparison between the results reported in Figure 13 shows that the specific absorbed energy of the empty complete corrugated tube LE-30 with an initial radius of 27.3 mm and a wall thickness of 0.5 mm is 9271 J/kg. Also, the specific absorbed energy of the preformed corrugated tubes LE-34 and LF-104 in the empty condition and the filled condition are 1521 J/kg and 1632 J/kg respectively. The corresponding values for the empty simple tube LE-42 and the filled simple tube LF-95 are 441 J/kg and 1621 J/kg respectively. On the basis of these results, it is found that the specific absorbed energy of the complete corrugated tube LE-30 with the empty condition is 6.09 times and 5.69 times the specific absorbed energies of the empty preformed corrugated tubes and the filled preformed corrugated tubes respectively with the same wall thicknesses and the same diameters. Also, the specific absorbed energy of the empty complete corrugated tube LE-30 is 21.02 times and 5.72 times the specific absorbed energies of the empty simple tubes and the filled simple tubes respectively. The recent comparison shows the considerable advantage of using the complete corrugated tubes as a desirable energy absorber system in the lateral compression loading condition.

Axial compression

Based on the experimental results in the quasi-static axial loading condition, the effects of the geometrical shape, the diameter, the wall thickness of the tubes and also the filler on the axial load and the energy absorption capability of the specimens are studied.

Effect of the tube form. Figure 15(a) compares the experimental curves of axial load versus axial displacement of specimens AE-7, AE-3 and AE-12 up to the same

displacement. These specimens have the same wall thicknesses and inner diameters, but specimen AE-7, specimen AE-3 and specimen AE-12 are a complete corrugated tube, a preformed corrugated tube and a circular tube respectively. Figure 15(a) shows that the required axial load for folding the circular tube is the highest, in comparison with that required for the corrugated specimens. This means that the complete corrugated tube has the lowest axial compression load, in comparison with those of the other specimens. Comparison of the areas under the load versus displacement curves, which shows the absorbed energy, indicates that, for specimens of the same materials, same nominal diameters and same wall thicknesses, but with different forms, simple circular tubes have the highest capability of energy absorption, and complete corrugated tubes have the lowest. Also, Figure 15(b) illustrates the absorbed energy versus displacement curves of the complete corrugated tube AF-62, the preformed corrugated tube AF-58 and the circular tube AF-67. All the specimens have the same wall thicknesses, same nominal diameters, same materials and same filling conditions, but they have different forms. Figure 15(b) shows that, for the polyurethane-foam-filled specimens, the simple tubes have the maximum energy absorption capability, in comparison with those of the corrugated specimens. Also, the minimum energy is absorbed by the complete corrugated tube.

In the design of an energy absorber, the specific absorbed energy is one of the main parameters. The specific absorbed energies of the complete corrugated tube AE-7, the preformed corrugated tube AE-3 and the simple tube AE-12 are 1421 J/kg, 3870 J/kg and 9478 J/kg respectively. Therefore, for specimens with a nominal radius of 27.3 mm, the specific absorbed energy of the simple tube is 2.45 times and 6.67 times the specific absorbed energies of the corresponding preformed corrugated tube and the complete corrugated tube respectively. Also, for specimens with a nominal radius of 55.4 mm, the energy-to-mass ratio of the simple tube AE-19 is 2.37 times and 14.6 times those of the similar preformed corrugated tube and the complete corrugated tube respectively. Therefore, from the crashworthiness viewpoint, in the quasi-static axial loading condition, simple tubes are preferred to corrugated specimens, but there are some advantages for corrugated specimens. The experimental observations show that, by shaping simple circular tubes into corrugated specimens, the controllability of the structure increases and, during the loading, the probability of the folding process as the desirable deformation mode increases. For example, when compressive loading is applied at a certain angle with respect to the tube axis, the probability of the folding deformation mode in corrugated tubes is greater than in simple tubes. Also, the experimental measurements and the load versus displacement curves in Figure 15(b) show that, when simple circular tubes are shaped into preformed or complete corrugated tubes by the hydroforming method, the maximum axial load of the initial parts of the folding process decreases markedly and, even in complete corrugated tubes, it is omitted. As a numerical example, the ratios of the peak load to the steady load of the simple circular tube AE-12, the preformed corrugated tube AE-3 and the complete corrugated tube AE-7 are 3.34, 1.65 and 1 respectively. Here, the steady load means the approximately constant load after the initial peak load. From the crashworthiness viewpoint, an energy absorber without an initial maximum load is an ideal system because, in this situation, the maximum applied load to the other parts of the structure decreases, which is a desirable phenomenon.

Effect of the diameter. Figure 16 illustrates the load versus displacement curves of the axial compression tests on specimens AE-1, AE-7 and AE-23. All these specimens are complete corrugated tubes and they have the

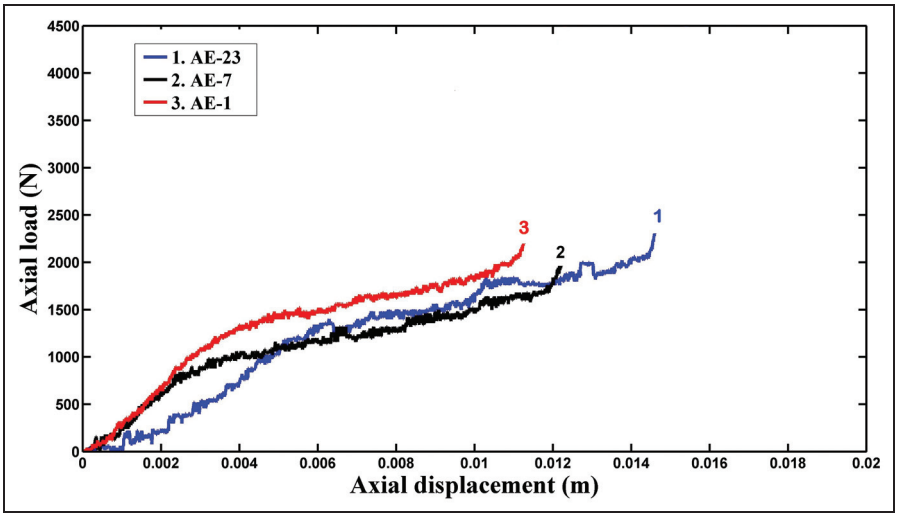

Figure 16. Axial load versus displacement curves of complete corrugated tubes with different diameters.

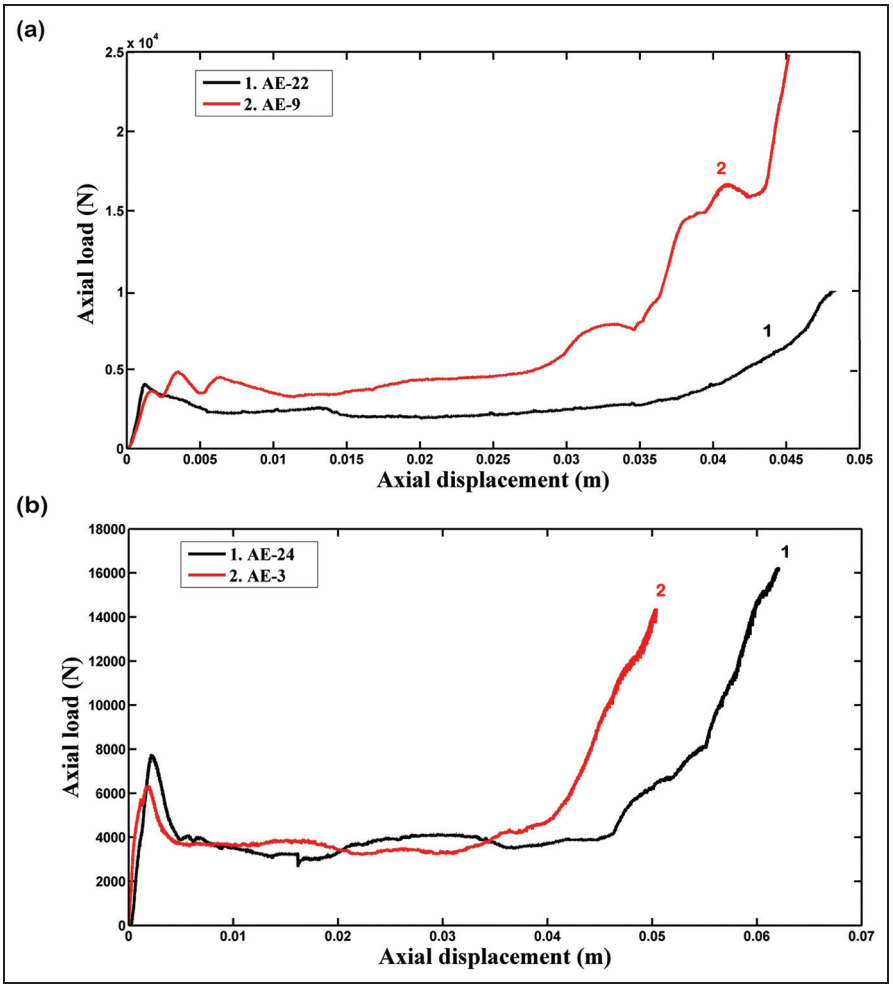

Figure 17. Axial load versus displacement diagrams of empty corrugated tubes with different diameters: (a) t = 0.4 mm; (b) t = 0.5 mm.

same wall thicknesses and material properties, but different diameters. The results show that the nominal diameter and the corrugation radii of specimen AE-7 are 24.1% and 7.3% larger than the corresponding values of specimen AE-1. Also, the specific absorbed energy of specimen AE-7 is 27.2% higher than the specific absorbed energy of specimen AE-1. Also, the nominal diameter and the corrugation radii of specimen AE-23 are 63.2% and 26.3% larger than those of specimen AE-1, but the specific absorbed energy of specimen AE-23 is 46.1% less than the specific absorbed energy of specimen AE-1. This means that the energy-absorption-to-mass ratio of the complete corrugated tubes is greatly dependent on the specimen diameter and the corrugation radii and, by changing the above-mentioned geometrical parameters, the optimum complete corrugated tube subjected to axial loading is obtained.

For polyurethane-foam-filled complete corrugated tubes, the specific absorbed energies of specimens AF-55, AF-62 and AF-76 with corresponding nominal radii of 22 mm, 27.3 mm and 35.9 mm are 3859 J/kg, 2997 J/kg and 585 J/kg respectively. On the other hand, for filled complete corrugated tubes, by increasing the specimen diameter, the specific absorbed energy decreases and so, in the studied cases, a filled specimen with a smaller diameter is a better energy absorber.

Diagrams of the axial load versus the axial displacement of two pairs of empty preformed corrugated tubes are illustrated in Figure 17. Figure 17(a) shows that, for the specimens with a wall thickness of 0.4 mm, the axial load of the tube with a smaller diameter is higher. Figure 17(b) shows that, for the preformed corrugated tubes with a wall thickness of 0.5 mm, the axial loads of the two specimens with nominal radii of 27.3 mm and 35.9 mm are near to each other. As a numerical study, the specific absorbed energy of specimen AE-9 with a radius of 22 mm is 1.92 times the specific absorbed energy of specimen AE-22 with a radius of 27.3 mm, and also the specific absorbed energy of specimen AE-3 with a nominal radius of 27.3 mm is 1.50 times the specific absorbed energy of the preformed corrugated tube AE-24 with an initial radius of 35.9 mm. This shows that, in the investigated cases, an empty preformed corrugated tube with a smaller diameter has a better performance.

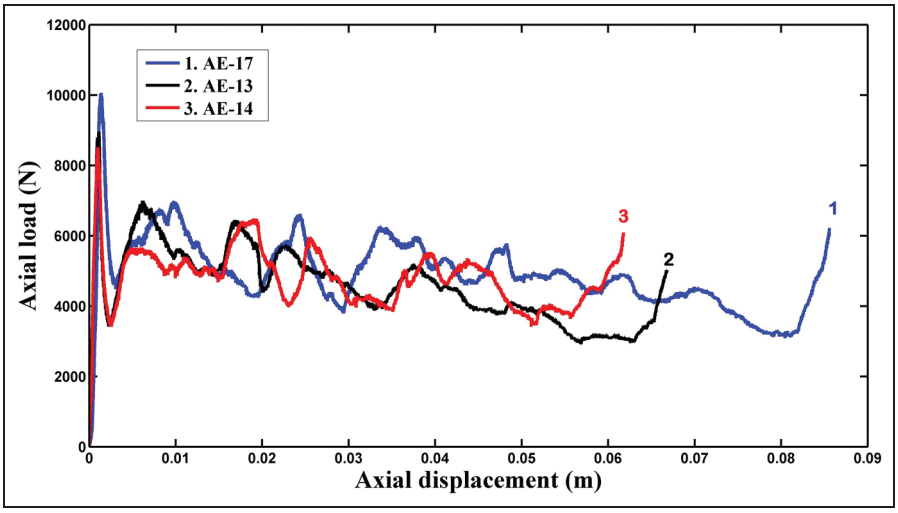

Figure 18. Axial load versus displacement diagrams of empty circular tubes with different diameters: (a) t = 0.4 mm; (b) t = 0.5 mm.

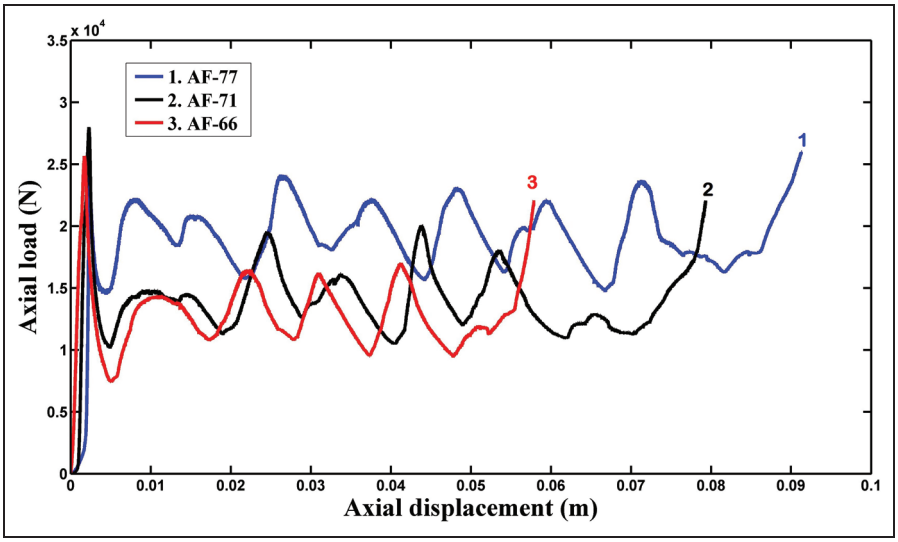

Figure 19. Axial load versus displacement curves of the simple filled tubes AF-66, AF-71 and AF-77 with different diameters.

The results show that the energy-to-mass ratio of the filled preformed corrugated tubes AF-58 and AF-57 with corresponding nominal radii of 27.3 mm and 35.9 mm and with the same materials and same wall thicknesses are 6762 J/kg and 4066 J/kg respectively. It is concluded that, by increasing the diameter of a filled preformed corrugated tube, the energy absorption performance of the structure decreases. The same results are obtained for the filled specimens AF-64 and AF-56.

Figure 18 compares the axial load versus displacement curves of the simple circular tubes with different diameters but with the other characteristics which are the same, in the empty condition. This figure shows that for empty simple tubes, by increasing the diameter, the initial peak load increases. Also, the specific absorbed energies of the circular tubes AE-14, AE-13 and AE-17 with corresponding initial radii of 22 mm, 27.3 mm and 35.9 mm are 9143 J/kg, 7234 J/kg and 6290 J/kg respectively. The diameter of specimen AE-14 is 0.61 times the diameter of specimen AE-17; however, the specific absorbed energy of specimen AE-14 is 1.45 times the corresponding value of specimen AE-17. Therefore, the experiments show that, for simple circular tubes under axial compression loading, when the tube diameter is reduced, the specific absorbed energy of the specimen increases. Thus, in the design of an axially compressed energy absorber, a circular tube with a smaller diameter is suggested.

A similar study is performed on simple circular tubes in the foam-filled condition under axial loading. Figure 19 illustrates the folding force versus displacement curves of the filled specimens AF-66, AF-71 and AF-77 with nominal radii of 27.3 mm, 35.9 mm and 55.4 mm respectively. According to the areas under the curves and considering the structure mass, the specific absorbed energies of specimens AF-66, AF-71 and AF-77 are 10078 J/kg, 8158 J/kg and 6433 J/kg respectively. This means that, in the filled condition similar to the

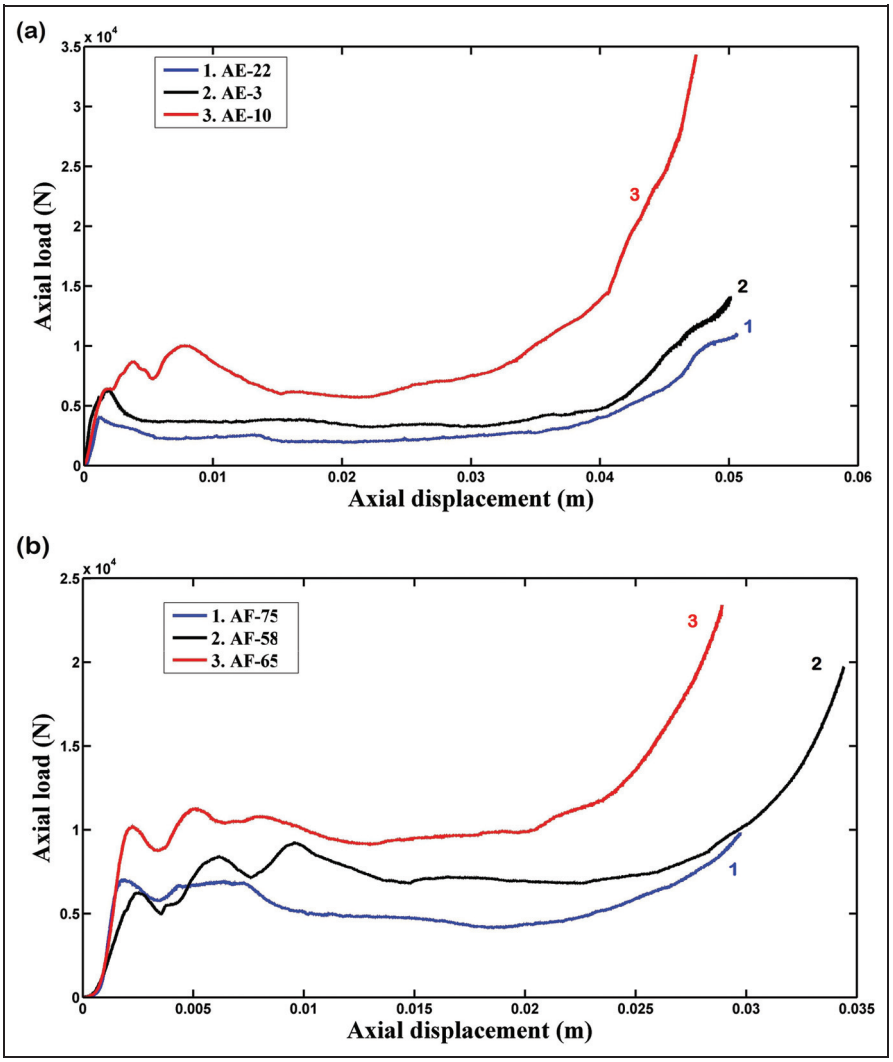

Figure 20. Axial load versus displacement diagrams of preformed corrugated tubes with different wall thicknesses: (a) empty; (b) foam filled.

situation in the empty condition, a circular tube with a smaller diameter has a better energy absorption behaviour.

Effect of the wall thickness. Curves of axial load versus displacement of the preformed corrugated tubes AE-22, AE-3 and AE-10 with the same material types and same diameters, but with different wall thicknesses are drawn in Figure 20(a). This figure shows that for empty preformed corrugated tubes, by increasing the wall thickness, the axial load also increases. The wall thicknesses of specimens AE-22, AE-3 and AE-10 are 0.4 mm, 0.5 mm and 0.6 mm respectively, and the specific absorbed energies of the specimens are 2058 J/kg, 3870 J/kg and 4103 J/kg respectively. This means that the wall thickness of specimen AE-3 is 1.25 times the wall thickness of specimen AE-22, while the specific absorbed energy of specimen AE-3 is 1.88 times the specific absorbed energy of specimen AE-22. Also, the wall thickness of specimen AE-10 is 1.2 times that of specimen AE-3, while the specific absorbed energy of specimen AE-10 is 1.06 times the specific absorbed energy of specimen AE-3. Therefore, although, by increasing the wall thickness of empty preformed corrugated tubes, the specific absorbed energy increases, there is an optimum value for the wall thickness, and the empty preformed corrugated tube with the optimized wall thickness has the best performance.

Also, Figure 20(b) demonstrates the axial load versus displacement curves of the polyurethane-foam-filled preformed corrugated tubes AF-75, AF-58 and AF-65 with wall thicknesses of 0.4 mm, 0.5 mm and 0.6 mm respectively and with the same materials and same nominal diameters. This figure shows that the order of the axial loads of filled tubes is similar to the order of their wall thicknesses. The experimental measurements demonstrate that the specific absorbed energies of specimens AF-75, AF-58 and AF-65 are 5529 J/kg, 6762 J/kg and 7637 J/kg respectively. This means that, for the filled condition of preformed corrugated tubes, a thicker tube has a more desirable performance. Therefore, although specimens with thicker walls have higher masses, the specific absorbed energy of a thicker

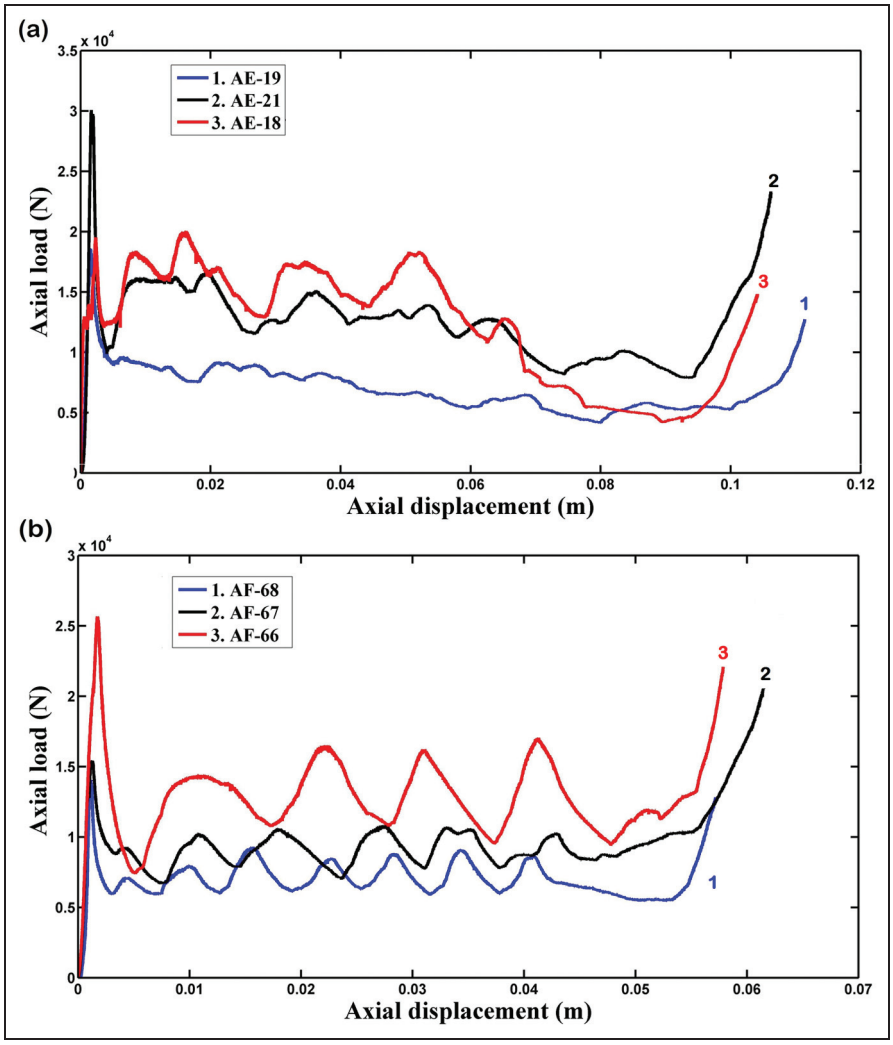

Figure 21. Axial load versus displacement diagrams of circular tubes with different wall thicknesses: (a) empty; (b) foam filled.

preformed corrugated tube is higher than that of a similar preformed corrugated tube with thinner walls.

Figure 21(a) and (b) illustrates the load versus displacement diagrams of the circular tubes in the empty condition and the foam-filled condition respectively. In each figure, the specimens have the same material types and same diameters, but different wall thicknesses. Comparison of the curves show that, in both the empty condition and the foam-filled condition of the simple circular tubes, there is an optimum value for the tube wall thickness, and the designed specimen with the optimum wall thickness is the best energy absorber. As a numerical investigation, the results show that the specific absorbed energies of the empty simple tubes AE-19, AE-21 and AE-18 are 4998 J/kg, 6908 J/kg and 5731 J/kg, and the specific absorbed energies of the filled simple tubes AF-68, AF-67 and AF-66 are 8045 J/kg, 1006 J/kg and 1008 J/kg respectively. The numerical comparison reaffirms the recent conclusion.

Effect of the foam filler. Comparison between the absorbed-energy-to-mass ratios of the empty specimens and the corresponding filled specimens is shown in Figure 22. In the first part of the figure, the simple circular tubes in the empty condition and the filled condition are compared. The figure shows that the specific absorbed energies of the empty simple circular tube AE-14 and the similar foam-filled specimen AF-69 are 9143 J/kg and 9273 J/kg respectively. According to Figure 22, it is found that, for the simple tubes, all the filled specimens have higher specific absorbed energies than those of the corresponding empty specimens, except for specimen AF-70 with an initial radius of 35.9 mm. This means that a simple tube in the polyurethane-foam-filled condition is usually a better choice, in comparison with a similar empty specimen.

The second part of the figure shows the specific absorbed energies of the preformed corrugated tubes during the folding process. As an example, Figure 22 shows that the preformed corrugated tube AF-58 in the foam-filled condition and the corresponding empty specimen AE-3 have absorbed-energy-to-mass ratios of 6762 J/kg and 3870 J/kg respectively. This shows an increase of 74.7% in the specific absorbed energy of the filled specimen. Also, the second part of the figure

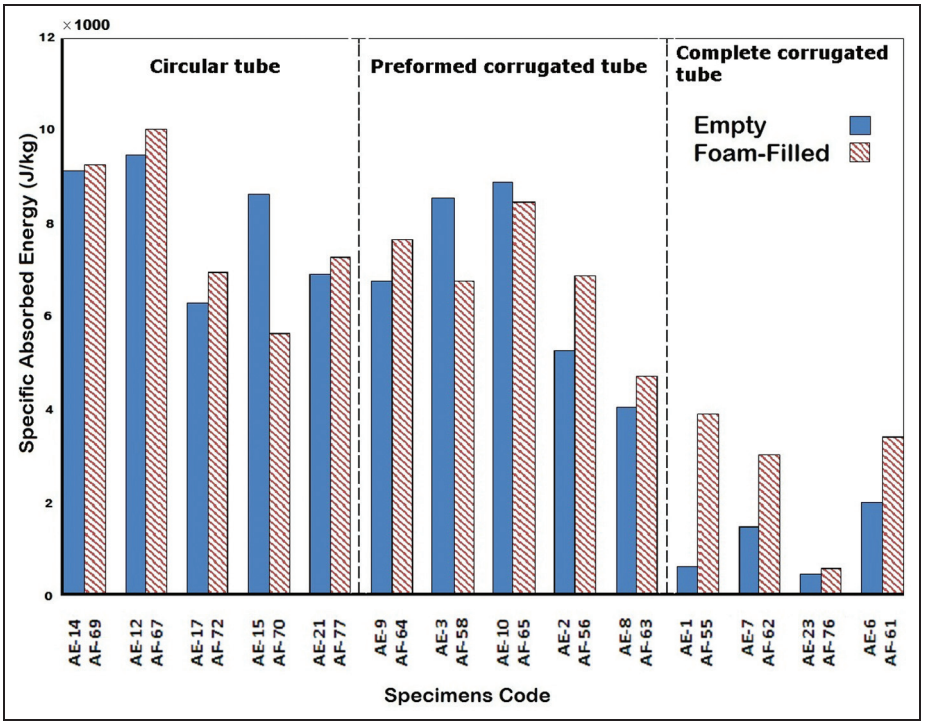

Figure 22. Comparison of the specific absorbed energies of the empty specimens and the corresponding polyurethane-foam-filled specimens under axial compression.

shows that in the same way as for simple circular tubes, in most cases of preformed corrugated tubes, by increasing the nominal diameter the specific absorbed energy decreases. Furthermore, it is found that for preformed corrugated tubes, by filling the specimens with polyurethane foam, the specific absorbed energy of the structure always increases, in comparison with those of similar empty specimens. As a numerical study, specimens AE-8 and AF-63 are preformed corrugated tubes with the same geometrical characteristics and the same material properties, but specimen AE-8 is empty and specimen AF-63 is foam filled. Figure 22 indicates that specimens AE-8 and AF-63 have specific absorbed energies of 4017 J/kg and 4690 J/kg respectively. The results show an increase of 16.8% in the specific absorbed energy of the filled tube. The second part of the figure shows that the polyurethane foam improves the performance of the preformed corrugated tubes from the viewpoint of the energy absorption behaviour, but this effectiveness usually decreases on increasing the inner diameter. This shows that, in preformed corrugated tubes with large diameters, the tube has a considerable share of the total absorbed energy of the structure.

The third part of Figure 22 compares the specific absorbed energies of the empty and the filled complete corrugated tubes. This figure shows that, for complete corrugated tubes, the filler has a significant influence on the energy absorption process. For example, the empty complete corrugated tube AE-1 and the foam-filled complete corrugated tube AF-55 have the same nominal diameters and the same material properties, and their specific absorbed energies are 561 J/kg and 3859 J/kg respectively. This means that, owing to the foam filler, the specific absorbed energy of the filled tube increases by 688%, in comparison with that of the empty tube. Although, for complete corrugated tubes, filling the specimens has considerable positive effects on the energy absorption trend, Figure 22 obviously shows large decreases in the specific absorbed energies of the corrugated tubes in comparison with those of the simple tubes, and this increases the cost of controlling the mode deformation. In other words, in simple circular tubes under axial loading, depending on the geometrical characteristics and the applied force angle with respect to the structure axis, two different deformation modes may occur: global buckling and folding. Although shaping the simple tubes into corrugated tubes reduces the energy absorption capacity, the deformation mode becomes more controllable.

An interesting conclusion is reached by comparing the specific absorbed energies of complete corrugated tubes, preformed corrugated tubes and simple circular tubes. Figure 22 shows that, by shaping a simple tube into a corrugated specimen, the specific absorbed energy of the specimen decreases but, by filling the corrugated specimen with polyurethane foam, the specific absorbed energy of the structure increases and can attain the same order of magnitude as those of simple circular tubes. Therefore, on axial loading, corrugated specimens in the polyurethane-foam-filled condition can be introduced as an energy absorber system with a controllable deformation mode and a high energy absorption capability.

By comparing the reported specific absorbed energies of the empty and filled specimens under lateral loading and axial loading respectively in Figures 13 and 22, it is found that, during the lateral compression tests (the flattening process), the specific absorbed energies of the complete corrugated tubes, the preformed corrugated tubes and the circular tubes are in the ranges 1672–12138 J/kg, 3487–7308 J/kg and 222–2002 J/kg respectively. Also, in the axial compression tests (the folding process), the specific absorbed energies of the complete corrugated tubes, the preformed corrugated tubes and the circular tubes are in the ranges 389–3859 J/kg, 3870–8467 J/kg and 5610–10062 J/kg respectively. Generally, the folding process under axial loading has a considerably higher specific absorbed energy than the flattening process under lateral loading has for similar specimens, and this has been reported in some previous published studies.[28, 29] However, in the present work, an interesting result is obtained. Comparison of the above-mentioned numerical results shows that, in some cases, the specific absorbed energies of the complete corrugated tubes under lateral loading are higher than the specific absorbed energies of the circular tubes under axial loading. This means that, by shaping simple circular tubes into preformed or complete corrugated tubes via the hydroforming process, a new thin-walled structure with a high specific absorbed energy during the flattening process in lateral compression tests is introduced. Thus, the present article suggests using a thin-walled corrugated tube as an energy absorber system with a high crashworthiness performance in the design of some parts of automobiles such as the bumper beam to enhance the vehicle safety.

Introduction of an energy absorption system with a desirable performance under different loading conditions has been one of the most interesting topics for researchers. By pressurizing the cellular materials, honeycombs or thin-walled structures, their energy absorption can be greatly enhanced, and this enhancement can be controlled by the applied pressure. This concept explains the possibility of achieving adaptive energy absorption. Zhang and Yu[30] presented a study on the axial crushing of pressurized thin-walled circular tubes to investigate the effect of the internal pressure on the energy absorption of thin-walled structures. Their investigation showed that the mean crushing force of the pressurized tube increased linearly with increasing internal pressure and that the energy absorption enhancement arises from two mechanisms: the direct effect of the pressure and the indirect effect caused by interaction between the pressure and the tube wall. However, this method is not advantageous and does not have sufficient safety in many conditions. Eyvazian et al.[26] performed an experimental investigation to study the responses of aluminium corrugated tubes with various corrugation geometries to quasi-static compressive loading in the axial direction. They showed that empty corrugated tubes under axial loading have low specific absorbed energies, in comparison with those of simple circular tubes. The present article introduces polyurethane foam as the filler into corrugated specimens to improve their specific absorbed energies under axial loading and also their energy absorption characteristics under lateral compression. The experiments show incredible results for corrugated tubes as energy absorbers under lateral compression. Li et al.[31] studied the crushing behaviour of empty tubes, foam-filled single tubes and double circular tubes subjected to quasi-static oblique loads experimentally. Their results showed the effectiveness of foam in oblique loads. However, in the present paper, Figures 13 and 22 precisely illustrate the positive and negative effects of filling the specimens in a wide range. As a result, filling the corrugated tubes under axial crushing with polyurethane foam is an intelligent method to obtain both controllability and high energy absorption capability.

Conclusion

This article investigates the energy absorption behaviour of empty and polyurethane-foam-filled circular tubes, preformed corrugated tubes and complete corrugated tubes during the lateral compression and the axial compression processes between two rigid platens by the experimental method. The results show that, through the flattening process on empty and polyurethane-foam-filled specimens, complete corrugated tubes have the highest specific absorbed energies, while the specific absorbed energies of simple tubes are the lowest. Also, for both empty and filled complete corrugated tubes, by increasing the diameter, the lateral compressive load is reduced, but the ultimate crushing displacement is increased. The results show that, in both the empty and the polyurethane-foam-filled conditions of complete corrugated tubes, the specimens with initial inner radii of 22.0 mm and 55.4 mm have higher CFEs than those of the other specimens, and it introduces some optimum diameters from the viewpoint of the CFE. Experimental investigation shows that, for corrugated tubes with polyurethane foam filler, increasing the tube wall thickness enhances the specific absorbed energies. The test results show that the required axial load of the folding process on circular tubes is the highest, in comparison with that required for corrugated specimens. For filled complete corrugated tubes under an axial load, by increasing the specimen diameter, the specific absorbed energy is decreased. Thus, in the studied cases, a filled specimen with a smaller diameter is a better energy absorber. However, for complete corrugated tubes subjected to axial loading, filling the specimens with polyurethane foam has considerable positive effects on the energy absorption trend of the structure.

Acknowledgements

The authors gratefully acknowledge the Iran Industrial Vibrations Company for its support in preparing the specimens, and Seyed Ali Elahi and Seyed Ghaem

Amirhosseini for their help in this research programme. Also, the authors gratefully acknowledge the Strength of Materials Laboratory at Yasouj University and Ezzatallah Hosseinzadeh.

Declaration of conflict of interest

The authors declare that there is no conflict of interest.

Funding

This research received no specific grant from any funding agency in the public, commercial or not-for-profit sectors.

References

1. Gupta NK and Velmurugan R.Consideration of internal folding and non-symmetric fold formation in axisymmetric axial collapse of round tubes. *Int J Solid Structs* 1996; 34: 2611–2630.
2. Wu EL and Carney JF.Experimental analyses of collapse behaviors of braced elliptical tubes under lateral compression. *Int J Mech Sci* 1998; 40: 761–777.
3. Niknejad A, Liaghat GH, Moslemi Naeini H and Behravesh AH.A theoretical formula for predicting the instantaneous folding force of the first fold in a single cell hexagonal honeycomb under axial loading. *Proc IMechE Part C: J Mechanical Engineering Science* 2010; 224: 2308–2315.
4. Guillow SR, Lu G and Grzebieta RH.Quasi-static axial compression of thin-walled circular aluminium tubes. *Int J Mech Sci* 2001; 43: 2103–2123.
5. Abramowicz W.Thin-walled structures as impact energy absorbers. *Thin-Walled Structs* 2003; 41: 91–107.
6. Huang X, Lu G and Yu TX.Collapse of square metal tubes in splitting and curling mode. *Proc IMechE Part C: J Mechanical Engineering Science* 2006; 220: 1–13.
7. Marsolek J and Reimerdes HG.Energy absorption of metallic cylindrical shells with induced non-axisymmetric folding patterns. *Int J Impact Engng* 2004; 30: 1209–1223.
8. Jones N and Birch RS.Dynamic and static axial crushing of axially stiffened square tubes. *Proc IMechE Part C: J Mechanical Engineering Science* 1990; 204: 293–310.
9. Mamalis AG, Manolakod E, Baldoukasj K and Viegelahn GL.Deformation characteristics of crashworthy thin-walled steel tubes subjected to bending. *Proc IMechE Part C: J Mechanical Engineering Science* 1989; 203: 411–417.
10. Morris E, Olabi AG and Hashmi MSJ. Analysis of nested tube type energy absorbers with different indenters and exterior constraints. *Thin-Walled Structs* 2006; 44: 872–885.
11. Olabi AG, Morris E and Hashmi MSJ. Metallic tube type energy absorbers: a synopsis. *Thin-Walled Structs* 2007; 45: 706–726.
12. Abdewi EF, Sulaiman S, Hamouda AMS and Mahdi E.Quasi-static axial and lateral crushing of radial corrugated composite tubes. *Thin-Walled Structs* 2008; 46: 320–332.
13. Mahdi ES and El Kadi H.Crushing behavior of laterally compressed composite elliptical tubes: experiments and predictions using artificial neural networks. *Composite Structs* 2008; 83: 399–412.
14. Aktay L, Kroplin BH, Toksoy AK and Guden M.Finite element and coupled finite element/smooth particle hydrodynamics modeling of the quasi-static crushing of empty and foam-filled single, bitubular and constraint hexagonal- and square-packed aluminum tubes. *Mater Des* 2008; 29: 952–962.
15. Olabi AG, Morris E, Hashmi MSJ and Gilchrist MD.Optimised design of nested circular tube energy absorbers under lateral impact loading. *Int J Mech Sci* 2008; 50: 104–116.
16. Poonaya S, Teeboonma U and Thinvongpituk C.Plastic collapse analysis of thin-walled circular tubes subjected to bending. *Thin-Walled Structs* 2009; 47: 637–645.
17. Niknejad A, Liaghat GH, Moslemi Naeini H and Behravesh A.Theoretical and experimental studies of the instantaneous folding force of the polyurethane foam-filled square honeycombs. *Mater Des* 2011; 32: 69–75.
18. Fan Z, Shen J and Lu G.Investigation of lateral crushing of sandwich tubes. *Procedia Engng* 2011; 14: 442–449.
19. Niknejad A, Elahi SA and Liaghat GH.Experimental investigation on the lateral compression in the foam-filled circular tubes. *Mater Des* 2012; 36: 24–34.
20. Niknejad A, Abedi MM, Liaghat GH and Zamani Nejad M.Prediction of the mean folding force during the axial compression in foam-filled grooved tubes by theoretical analysis. *Mater Des* 2012; 37: 144–151.
21. Mahdi E and Hamouda AMS. Energy absorption capability of composite hexagonal ring systems. *Mater Des* 2012; 34: 201–210.
22. Obradovic J, Boria S and Belingardi G.Lightweight design and crash analysis of composite frontal impact energy absorbing structures. *Composite Structs* 2012; 94: 423–430.
23. Alavi Nia A and Parsapour M. An investigation on the energy absorption characteristics of multi-cell square tubes. *Thin-Walled Structs* 2013; 68: 26–34.
24. Martinez G, Graciano C and Teixeira P.Energy absorption of axially crushed expanded metal tubes. *Thin-Walled Structs* 2013; 71: 134–146.
25. Mahdi E, Hamouda AMS and Sebaey TA.The effect of fiber orientation on the energy absorption capability of axially crushed composite tubes. *Mater Des* 2014; 56: 923–928.
26. Eyvazian A, Habibi MK, Hamouda AM and Hedayati R.Axial crushing behavior and energy absorption efficiency of corrugated tubes. *Mater Des* 2014; 54: 1028–1038.
27. Hong W, Fan H, Xia Z et al. Axial crushing behaviors of multi-cell tubes with triangular lattices. *Int J Impact Engng* 2014; 63: 106–117.
28. Alghamdi AAA. Collapsible impact energy absorbers: an overview. *Thin-Walled Structs* 2001; 39: 189–213.
29. Reid SR.Metal tubes as impact energy absorbers. In: Reid SR (ed) *Metal forming and impact mechanics*. Oxford: Pergamon Press, 1985, pp. 249–269.
30. Zhang XW and Yu TX.Energy absorption of pressurized thin-walled circular tubes under axial crushing. *Int J Mech Sci* 2009; 51: 335–349.
31. Li Z, Yu J and Guo L.Deformation and energy absorption of aluminum foam-filled tubes subjected to oblique loading. *Int J Mech Sci* 2012; 54: 48–56.